



PONTIFICIA UNIVERSIDAD CATOLICA DE CHILE  
ESCUELA DE INGENIERIA

**STRATIFIED CONCRETE: UNDERSTANDING  
ITS STRATIFICATION PROCESS AND  
MODELLING ITS STRUCTURAL BEHAVIOR**

**IVÁN IGNACIO NAVARRETE LESCHOT**

Thesis submitted to the Office of Research and Graduate Studies in partial fulfillment of the requirements for the Degree of Master of Science in Engineering

Advisor:

**MAURICIO LÓPEZ CASANOVA**

Santiago de Chile, November, 2015

© MMXV, Iván Ignacio Navarrete Leschot



PONTIFICIA UNIVERSIDAD CATOLICA DE CHILE  
ESCUELA DE INGENIERIA

# **STRATIFIED CONCRETE: UNDERSTANDING ITS STRATIFICATION PROCESS AND MODELLING ITS STRUCTURAL BEHAVIOR**

**IVÁN IGNACIO NAVARRETE LESCHOT**

Members of the Committee:

**MAURICIO LÓPEZ CASANOVA**

**MATÍAS HUBE GINESTAR**

**RICARDO SERPELL CARRIQUIRY**

**JAVIER CASTRO SEPULVEDA**

**GUILLERMO THENOUX ZEBALLOS**

Thesis submitted to the Office of Research and Graduate Studies in partial fulfillment of the requirements for the Degree of Master of Science in Engineering

Santiago de Chile, November, 2015

*To my family and friends*

## ACKNOWLEDGMENTS

I would like to thank my family for their continuous support and encouragement during this process. I would like to dedicate my thesis to my mother, my father, my sister, my girlfriend, my aunt Marisa and my grandmother Angela. Thank you all for your support, trust and love.

I also would like to thank my advisor, Professor Mauricio López, for his guidance and advice during these research process. I want to acknowledge the assistance and commentaries of Professors Yahya Kurama and Matías Hube.

I also wish to thank to ETC research group: José Carlos Remesar, Felipe Vargas, Ricardo Serpell, Felipe Rivera, Claudia Stuckrath, Melissa Soto, Franco Zunino and María Renee Oliva. I acknowledge the help of Mauricio Guerra, Luis Felipe Gonzalez and Patricio Pinilla for their assistance during the experimental work. I also acknowledge the advice of friends and classmates during this process, especially to Kaitlyn Dietz and Denisse Laux for their language support.

I also thank to Professors Guillermo Thenoux and Javier Castro for their advice as members of the committee. In addition, I recognize Cementos Melon, DICTUC S.A. and Sika for their contributions to this research project.

I gratefully acknowledge the funding provided by CONICYT/FONDEF D10I1086 and CONICYT-PCHA/MagisterNacional/2015 - 22150974.

## TABLE OF CONTENTS

ACKNOWLEDGMENTS .....	iii
TABLE OF CONTENTS .....	iv
LIST OF FIGURES .....	vii
LIST OF TABLES .....	ix
ABSTRACT .....	xi
RESUMEN.....	xiii
1. STRUCTURE OF THESIS .....	1
2. INTRODUCTION .....	2
2.1. Stratified Concrete .....	3
2.2. Rheology of concrete effect on segregation.....	7
2.3. Coarse aggregate effect on segregation.....	11
2.4. Vibratory energy effect on segregation.....	14
3. SUMMARY OF CONDUCTED WORK.....	17
3.1. Research Gap .....	17
3.2. Hypotheses .....	18
3.2.1. Hypothesis 1 .....	18
3.2.2. Hypothesis 2 .....	18
3.2.3. Hypothesis 3 .....	18
3.3. Objectives.....	19
3.4. Methodology .....	20
4. UNDERSTANDING THE RELATIONSHIP BETWEEN THE STABILITY OF CONCRETE UNDER VIBRATION AND COARSE AGGREGATE DENSITY AND SIZE .....	21
4.1. Introduction.....	22
4.2. Research Significance .....	25

4.3.	Materials and Methods .....	25
4.3.1.	Materials properties and mixture proportion .....	25
4.3.2.	Segregation measurement .....	27
4.4.	Results and Discussions .....	29
4.4.1.	Preliminary Mortar Characterization .....	29
4.4.2.	Limit for acceptable volumetric index .....	30
4.4.3.	Segregation rate .....	31
4.4.4.	R <sub>SSA</sub> value vs aggregate size .....	33
4.4.5.	Linear regression model for segregation rate .....	34
4.4.6.	Validation of the linear regression modelling of segregation rate .....	38
4.5.	Conclusions .....	40
5.	<b>ESTIMATING THE SEGREGATION OF CONCRETE BASED ON MIXTURE DESIGN AND VIBRATORY ENERGY .....</b>	<b>42</b>
5.1.	Introduction .....	43
5.2.	Research Significance .....	46
5.3.	Materials and Methods .....	46
5.3.1.	Materials properties and mixture proportion .....	46
5.3.2.	Segregation measurement .....	49
5.4.	Results and Discussions .....	51
5.4.1.	Relationship between mixture design parameters, energy applied and dynamic segregation .....	51
5.4.2.	Segregation degree .....	57
5.4.3.	Validation of MLR model for segregation .....	59
5.5.	Conclusions .....	62
6.	<b>STRATIFIED CONCRETE: CONSTRUCTION, FLEXURAL BEHAVIOR, ANALYSIS AND DESIGN APPROACH .....</b>	<b>64</b>
6.1.	Introduction .....	65
6.2.	Research Significance .....	67
6.3.	Research program .....	68
6.3.1.	Experimental program .....	68
6.3.2.	Analytical modelling .....	73
6.4.	Results and Discussions .....	75
6.4.1.	Stratified concrete layers properties .....	75

6.4.2. Experimental study .....	77
6.4.3. Analytical Study .....	81
6.5. Stratified concrete rectangular stress-block .....	83
6.6. Conclusions .....	87
7. CONCLUSIONS AND RECOMENDATIONS .....	89
7.1. Conclusions .....	89
7.2. Recommendations .....	91
REFERENCES .....	93
8. APPENDICES .....	101
8.1. Images of laboratory equipment.....	101
8.2. Volumetric Index measurement procedure .....	102
8.3. Fiber-element model of flexural behavior of reinforced stratified concrete .....	104
8.4. Monotonic load test in RSC specimens .....	110

## LIST OF FIGURES

Figure 2-1: Stabilizing effect of thermal mass on internal temperature.....	4
Figure 2-2: Building process of precast stratified concrete panels system. ....	5
Figure 2-3: Ideal rheological zone for stratification .....	5
Figure 2-4: Cylinders samples vibrated for 0, 15, 30 and 45 seconds .....	6
Figure 2-5: Schematic of shear stress versus strain rate curves for Bingham plastic materials .....	10
Figure 2-6: Sample results from scintillation camera experiment. ....	10
Figure 2-7: Variation between SC values with slump flow and V-time .....	11
Figure 2-8: Aggregate settlement vs. time .....	15
Figure 2-9: Effect of vibration amplitude and frequency in concrete segregation .....	16
Figure 4-1: Test specimens with a VI lower than 20% .....	30
Figure 4-2: Test specimens with a VI higher than 30% .....	31
Figure 4-3: Effect of $R_{SSA}$ value on segregation rate.....	36
Figure 4-4: Effect of $ \Delta\rho $ value on segregation rate. ....	36
Figure 4-5: Linear regression modelling and experimental results of segregation rate ...	39
Figure 5-1: Effect of vibratory energy on segregation of mixtures with same mortar V-time.....	56
Figure 5-2: Effect of vibratory energy on segregation of mixtures with same aggregate properties.....	57
Figure 5-3: Test specimens of EP-M1 mixture with different VI values.....	58
Figure 5-4: Experimental vs predicted results of VI values of Series II mixtures. ....	61
Figure 6-1: General and cross-sectional views of the test elements. ....	70
Figure 6-2: Plan view of elements with the vibration points for stratification .....	71
Figure 6-3: Test-setup used for flexural load test. ....	73
Figure 6-4: Fiber element model of reinforced stratified concrete elements .....	74
Figure 6-5: Cross-section of tested elements .....	75
Figure 6-6: Average segregation profile for SCS and SCG elements.....	76

Figure 6-7: Typical failure modes and crack patterns of flexural tests .....	78
Figure 6-8: Load-deflection curves of RSC .....	79
Figure 6-9: Comparison Analytical prediction and Experimental load-deflection curves .....	82
Figure 6-10: Stress and strain distribution for ORC elements .....	84
Figure 8-1: Vibratory table and accelerometer .....	101
Figure 8-2: Mortar V-funnel Test .....	101
Figure 8-3: Example of saw-cut of cylinder sample .....	102
Figure 8-4: Example of saw-cut of cylinder sample with point's grid. ....	102
Figure 8-5: Monotonic load test set up .....	110
Figure 8-6: Failure mode SCG-1 specimen .....	111
Figure 8-7: Load-deflection curve SCG-1 specimen .....	111
Figure 8-8: Failure mode SCG-2 specimen .....	112
Figure 8-9: Load-deflection curve SCG-2 specimen .....	112
Figure 8-10: Failure mode SCS-1 specimen .....	113
Figure 8-11: Load-deflection curve SCS-1 specimen.....	113
Figure 8-12: Failure mode SCS-1 specimen .....	114
Figure 8-13: Load-deflection curve SCS-1 specimen.....	114

## LIST OF TABLES

Table 4-1: Physical properties of single-sized aggregates .....	26
Table 4-2: Concrete mixture proportions .....	27
Table 4-3: Mortar mixture proportioning.....	29
Table 4-4: Aggregate parameters and stratification coefficients of series I concrete mixtures .....	32
Table 4-5: Segregation rate of concrete mixtures .....	33
Table 4-6: First proposed model summary and coefficient results of the segregation rate regression analysis.....	35
Table 4-7: Second proposed model summary and coefficient results of the segregation rate regression analysis.....	37
Table 4-8: Third proposed model summary and coefficient results of the segregation rate regression analysis.....	38
Table 4-9: Aggregate parameters and stratification coefficients of series II concrete mixtures .....	39
Table 5-1: Physical properties of single-sized aggregates .....	47
Table 5-2: Mortars V-time and HRWA doses .....	48
Table 5-3: Concrete mixture proportions .....	49
Table 5-4: Energy rate by mass applying by each maximum acceleration of the vibratory table .....	50
Table 5-5: vibrations times applied to achieve the same amount of energy applied by mass with different maximum acceleration of vibratory table.....	50
Table 5-6: Aggregate parameters and volumetric index (VI) of series I concrete mixtures .....	53
Table 5-7: Model summary and coefficient results of the VI values regression analysis	55
Table 5-8: VI range of segregation degrees .....	58
Table 5-9: Aggregate parameters of concretes of series II .....	60
Table 5-10 Experimental and predicted segregation results of mixture of series II .....	60

Table 6-1: Coarse aggregate properties.....68

Table 6-2: Concrete mixture proportions .....69

Table 6-3: Mixing protocol for stratified concrete mixtures.....71

Table 6-4: Summary of stratified concrete layers properties .....76

Table 6-5: Summary of load test results on RSC.....79

Table 6-6: Summary of Analytical prediction of load test results and corresponding errors.....82

Table 6-7: Comparison between rectangular stress-block method and experimental test results. ....86

## ABSTRACT

Energy efficient concrete houses demand cement based materials with reduced thermal conductivity. Stratified concrete is produced from a single concrete mixture which is vibrated to get a lightweight insulating layer and a normal-weight structural layer. The use of precast panel systems offers the opportunity to control the vibration process, which is necessary to achieve a correct stratification. Nevertheless, when the panel is lifted, the dead-weight of it induces flexural stresses that may exceed in-place construction values.

This research is divided in two sections: the first section studies the combined effect of mixture design parameters and vibration characteristics on segregation. The second section focus on assessing the flexural behavior for analysis and design of reinforced stratified concrete (RSC).

A segregation model was assessed to evaluate the effect of mixture design factors and vibration characteristics. It was concluded that the concrete mixture design parameters are more relevant to control the segregation tendency than the vibration characteristics. Also, the rate of segregation is an intrinsic property of concrete and it is independent of the vibration time applied.

Flexural tests results suggest that RSC present similar damage mode and different failure mode than ordinary reinforced concrete (ORC). The fiber element model accurately predicts the flexural behavior of RSC while the rectangular stress-block method underestimates the flexural strength of RSC by 26%, which is similar that obtained for ORC. Therefore, stratified concrete specimens can be correctly design using both, fiber element model and rectangular stress-block method, approaches.

Keywords: Stratified concrete, fresh concrete, vibration, aggregate size, aggregate density, segregation rate, vibratory energy, rheology, flexural strength, fiber element model, segregation, lightweight concrete, rectangular stress-block method, stereology analysis, concrete ductility,

## RESUMEN

En vías de aumentar la eficiencia energética de las casas, la conductividad térmica del hormigón debe reducirse. El hormigón estratificado es producido a partir de una mezcla que es vibrada para obtener una capa liviana aislante y otra de peso normal estructural. El uso de paneles prefabricados ofrece la oportunidad de controlar el proceso de vibrado, esto es necesario para lograr una estratificación correcta. Sin embargo, cuando el panel es levantado, su peso propio induce tensiones por flexión que pueden superar los esfuerzos a los que será sometida la construcción.

Esta investigación se divide en dos secciones: la primera sección estudia el efecto combinado de parámetros de diseño de mezcla de hormigón y características de la vibración en la segregación. La segunda sección se enfoca en el entendimiento del comportamiento a flexión para diseño y análisis de hormigón estratificado reforzado (RSC).

Un modelo analítico de segregación fue desarrollado para evaluar el efecto de los parámetros de diseño de mezcla y las características de la vibración. Se concluyó que los parámetros de diseño de mezcla son más relevantes que las características de la vibración para controlar la segregabilidad. Además, la tasa de segregación es una propiedad intrínseca del hormigón y es independiente del tiempo de vibrado.

Los resultados de flexión sugieren que el RSC presenta un modo de daño similar y un modo de falla distinto que el hormigón convencional reforzado (ORC). El modelo de fibras predice de manera precisa el comportamiento a flexión del RSC mientras que el método de rectángulo equivalente de tensiones subestima la resistencia a flexión por un 26%, lo cual es similar a lo obtenido para ORC. Por lo tanto, los elementos de hormigón estratificado pueden ser diseñados correctamente usando ambas, modelo de elementos fibras y método del rectángulo de tensiones equivalente, aproximaciones.

Palabras clave: Hormigón estratificado, hormigón fresco, vibración, tamaño del agregado, densidad del agregado, energía de vibración, reología, resistencia a flexión, modelo de elemento fibra, hormigón liviano, rectángulo equivalente de tensiones, análisis estereológico, ductilidad.

## **1. STRUCTURE OF THESIS**

Chapter Two presents an introduction of the state of the art of stratified concrete and segregation of concrete. The chapter describe stratified concrete and analyzes the relationship between concrete segregation, mixture design and vibration process. Chapter Three presents the knowledge gap identified from the state of the art. It also includes the hypothesis, objectives and methodology.

Chapter Four, Five and Six presents three articles that are going to be submitted to ISI journals. Chapter Four analyses the effect of volume-to-surface area of coarse aggregate and density difference between mortar and coarse aggregate in segregation of concrete during vibration. Chapter Five aims to understand and assess the effect and interaction of the aggregate parameters studied in Chapter Four, mortar viscosity and energy applied during vibration in the segregation of concrete. Chapter Six analyses the flexural behavior, modelling and design of reinforced stratified concrete specimens. Chapter Seven presents the conclusions and recommendations generated from the research.

## 2. INTRODUCTION

Nowadays, environmental impact and energy consumption have become concerns around the world. If we follow the current path, greenhouse gas and energy-related CO<sub>2</sub> emissions from 2005 to 2050 will rise by 52% and 78% respectively (OECD, 2009). On the other hand, space heating and cooling of residential sector account over 10% of total primary energy consumption (Corporación de Desarrollo Tecnológico, 2010; Pérez-Lombard, Ortiz, & Pout, 2008). The thermal performance of the building envelope is the main factor affecting its energy consumption (Fang, Li, Li, Luo, & Huang, 2014). Therefore, the thermal performance must be considered as important as the mechanical performance in building's design. Concrete, the most used construction material, excels in mechanical properties and constructability, but lacks in thermal resistance.

Thermal insulation for concrete wall houses is required by building codes in most populated areas of Chile (MINVU, 2011), Europe (EURIMA, 2007) and United States (Kibert, 2012). Concrete houses with walls of 15 cm width in Santiago, Chile demand a thermal conductivity of 0.42 W/mK, whereas the thermal conductivity of conventional concrete ranges between 1.4 W/mK and 2.3 W/mK (Kim, Jeon, Kim, & Yang, 2003). This has limited the market share of concrete home building systems. The required thermal insulation increases the direct costs and limits its use compared to other construction systems.

Stratified Concrete is produced from a single concrete mixture which is controlled segregated by vibration to produce a normal-weight concrete layer and a lightweight concrete layer. Normal-weight concrete provides the benefit of high compressive strength and thermal mass but has little insulating ability. On the other hand, lightweight concrete offers limited compressive strength and thermal mass but has excellent insulating properties due to its high air content (Chandra & Berntsson, 2003). Building envelopes composed by both layers optimize thermal performance and reduce energy

consumption (Saevarsdottir, 2008). The literature review was focused on stratified concrete building process, fresh and hardened properties. Also, the effect of mixture design and vibration characteristics in segregation was studied to understand the stratification process.

## **2.1. Stratified Concrete**

The concept of stratified concrete was suggested by previous researchers (Bellamy & McSaveney, 2003). Stratified concrete specimens are made by combining two different concrete layers. To achieve this, a single mix containing both lightweight and normal-weight aggregate is cast and vibrated within the formwork to produce a controlled segregation. This process forms a normal-weight concrete (NWC) layer and a lightweight concrete (LWC) layer.

NWC provides the benefit of thermal mass but has little insulating ability. LWC in comparison offers limited thermal mass but has excellent insulating properties due to its low density and high air content (Kim et al., 2003; Sengul, Azizi, Karaosmanoglu, & Tasdemir, 2011; Yang & Li, 2008). Other important properties of the LWC layer include good sound insulation (Lesovik, Botsman, Tarasenko, & Botsman, 2014; Sousa, Carvalho, & Melo, 2004) as well as reduced energy demand during construction. Building envelope comprising both these layers can provide both thermal mass and insulating properties, leading to a considerable reduction in heating and cooling costs (Mackechnie, Saevarsdottir, & Bellamy, 2007).

Thermal mass is a property of the material that enables it to absorb and store thermal energy within its mass. This means that the concrete will absorb heat when the room is hot, store it, and then release it once the internal temperature drops below that of the concrete (Yang & Li, 2008). This results in cooler feeling rooms in summer and warmer rooms in winter. This means the temperature spikes are removed; interior temperature remains within a comfortable living temperature (Cement Concrete &

Aggregates Australia, 2002). Figure 2-1 shows how internal temperatures can be moderated with the use of thermal mass.

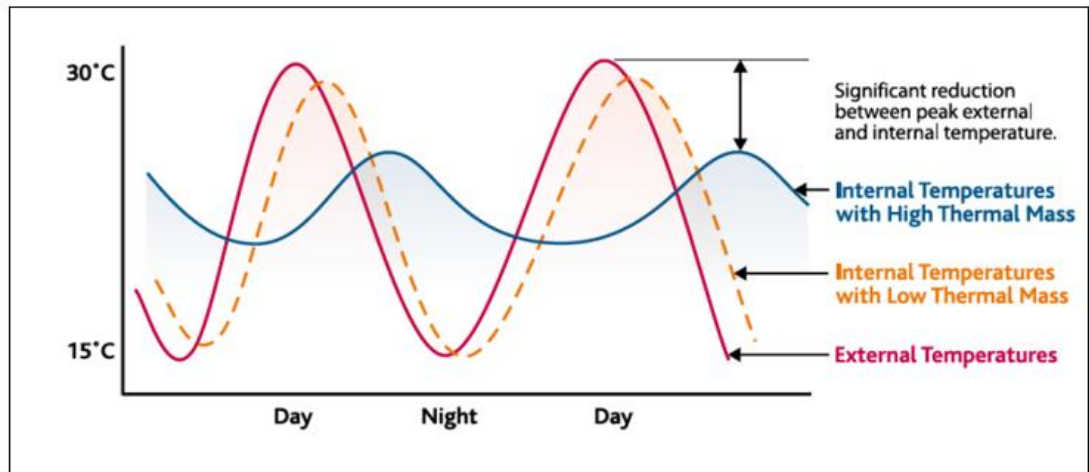


Figure 2-1: Stabilizing effect of thermal mass on internal temperature (The Concrete Centre, 2007)

Precast stratified concrete panel system for construction of residential homes envelope was proposed by previous researchers (Grange, 2012; Mackechnie et al., 2007). The use of precast panel systems offers the opportunity to control the quality of the end product to a very high degree, because the panels are supplied from specialized precasting factories and therefore cast in controlled environment (National Precast Concrete Association, 2006). This fact is very important for stratified concrete specimens, due to the vibration process must be controlled to achieve a correct stratification.

The building process of precast stratified concrete panels walls was proposed by Grange (2012) and the three main stage are summarized in Figure 2-2. The homogeneous concrete mixture is cast in one pour in a slab formwork where is vibrated to produce the stratification. Then, after setting and curing process, stratified concrete panel is transported to the construction site and lifted into place.

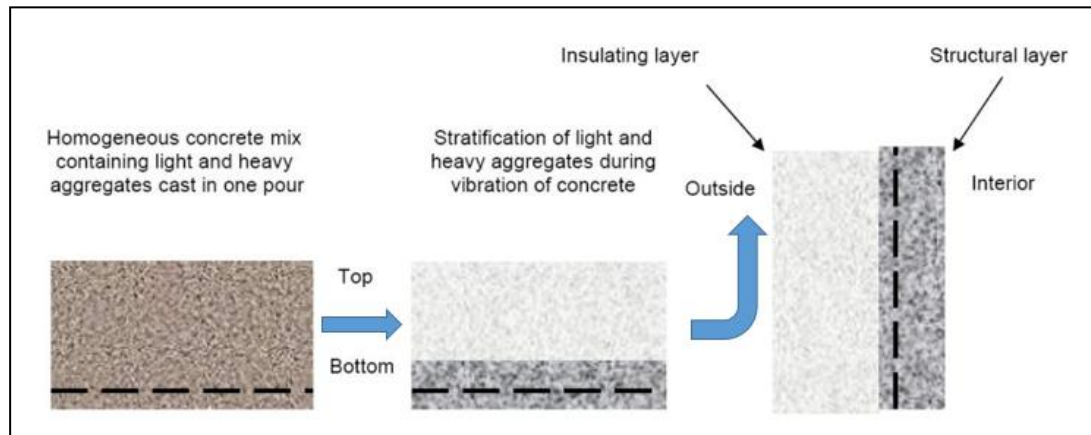


Figure 2-2: Building process of precast stratified concrete panels system (Grange, 2012).

Rheological testing have been carried out to locate the optimum zone for controlled segregation. Initial work suggested that a moderately cohesive concrete with good flow characteristics could produce a well stratified concrete (Mackechnie, Bellamy, & McSaveney, 2009). Figure 2-3 shows the rheological range for controlled stratification proposed by Mackechnie *et al.* When the plastic viscosity is too low, uncontrolled segregation can occurs during handling and the mix will separate. When it is too high, stratification is unlikely to occur as the mix provides resistance to any segregation.

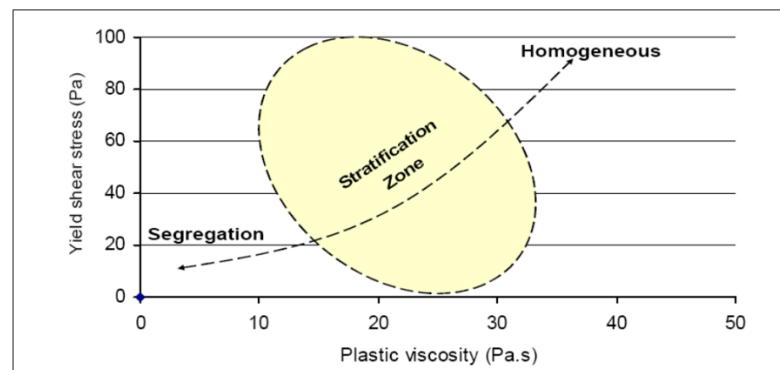


Figure 2-3: Ideal rheological zone for stratification (Mackechnie et al., 2009)

Stratification of concrete is dependent on the intensity and vibration time. By increasing the vibration time, more stratification is gained as Figure 2-4 display. A vibration time too short produced poorly stratified samples and a vibration time too long produced over stratified sample, i.e. the lightweight top layer lose paste (Mackechnie et al., 2007). On the other hand, Grange tested concrete mixtures with different coarse aggregate types and found that the time require to achieve an appropriate stratification is related to the aggregate density and size (Grange, 2012).



Figure 2-4: Cylinders samples vibrated for 0, 15, 30 and 45 seconds. (Mackechnie et al., 2007)

The degree of stratification is mainly dependent on the intensity and time of the vibration (Saevarsdottir, 2008), the rheological properties of mortar (Mackechnie et al., 2009) and the aggregate properties (Grange, 2012). However, there is a lack of understanding the combined effect or interaction of this factors in stratification.

The hardened properties of stratified concrete have been studied by previous researchers (Bellamy & McSaveney, 2003; Grange, 2012; Mackechnie et al., 2007; Mackechnie & Saevarsdottir, 2007; Saevarsdottir, 2008). Mackechnie and Saevarsdottir reported that stratified concrete samples of 25 cm width have a thermal resistance between 0.8 and 1.0 m<sup>2</sup>K/W (Mackechnie & Saevarsdottir, 2007). Considering the thermal insulation require for Chilean building code (MINVU,

2011), the stratified concrete studied by Mackechnie *et al* can be used between Arica and Chaiten. Saevarsdottir studied the flexural and axial compression strength of unreinforced laboratory samples (Saevarsdottir, 2008). He propose Eq. 1 to calculate the stratified concrete compressive strength.

$$f'_{c-SC} = \frac{w_{lwc} \cdot f'_{c-lwc} + w_{nwc} \cdot f'_{c-nwc}}{w_{lwc} + w_{nwc}} \quad (1)$$

Where  $f'_{c-SC}$ ,  $f'_{c-lwc}$  and  $f'_{c-nwc}$  are the compressive strength of stratified concrete, LWC layer and NWC layer, respectively; and  $w_{lwc}$  and  $w_{nwc}$  are the width of LWC and NWC layer, respectively. To the authors knowledge there are not previous studies focused in the understanding of mechanical behavior of full-scale reinforced stratified concrete specimens.

## 2.2. Rheology of concrete effect on segregation

The rheology of fresh concrete is complex due to its composition and the accompanying chemical changes. Previous researchers have described fresh concrete as a complex non-Newtonian material that possesses a yield stress and a shear rate dependent viscosity. Both the yield stress and the viscosity change with time (Ferraris, 1999; Larrard et al., 1997; Tattersall & Baker, 1988; Tattersall & Banfill, 1983). As the concrete sets, the yield stress and the viscosity increase greatly. In practice, the flow behavior of fresh concrete is simply represented by the Bingham model (Equation 2) (P. F. Banfill, 2006; Tattersall & Banfill, 1983).

$$\tau = \tau_0 + \eta_p \cdot \dot{\gamma} \quad (2)$$

Where  $\tau$  is the shear stress,  $\tau_0$  is the yield stress,  $\dot{\gamma}$  is shear rate, and  $\eta_p$  is the plastic viscosity.

Fresh concrete may be considered as a two-phase composite material with coarse aggregate particles in a continuous mortar matrix. Beris *et al.* predicted that a spherical particle (i.e. coarse aggregate) would settle in a fluid with Bingham plastic behavior (i.e. mortar matrix) only when the yield stress parameter, defined in Eq. 3, is less than 0.143, assuming the spherical particle has a higher density than the fluid (Beris, Tsamopoulos, Armstrong, & Brown, 1985).

$$Y_g = \frac{3 \cdot \tau_0}{2 \cdot R \cdot (\rho_s - \rho_f) \cdot g} \quad (3)$$

Where R is radius of a sphere;  $(\rho_s - \rho_f)$  is the density difference between the sphere and fluid; and g is the acceleration due to gravity. Once the settlement starts, the movement of a spherical particle in a Bingham fluid may be derived from Stokes drag (Petrou, Wan, Gadala-Maria, Kolli, & Harries, 2000), defined in Eq. 4.

$$U = \frac{2 \cdot R^2 \cdot (\rho_s - \rho_f) \cdot g}{9 \cdot \eta_p \cdot C_s} \quad (4)$$

Where U is the velocity of movement in the fluid of the sphere and  $C_s$  is the Stokes drag coefficient.

From Eq. 3 and Eq. 4 it is apparent that in fresh concrete the start of movement of the aggregate particles depends on the yield stress of the mortar, the density difference between the aggregate particles and the mortar matrix, and the size of the coarse aggregate. Once movement occurs, the velocity of the movement is affected by the plastic viscosity of the mortar in addition to the density difference between the coarse aggregate particle and the mortar and the size of the coarse aggregate.

When fresh concrete is subjected to vibration, previous researchers (Kakuta & Kojima, 1989; Larrard et al., 1997; Tattersall & Baker, 1988; Tattersall & Banfill, 1983) observed significant changes in its rheological properties. Some researchers

(Kakuta & Kojima, 1989; Tattersall & Baker, 1988) found that, under vibration, the plastic viscosity of concrete changes and the concrete become shear-thinning. de Larrard *et al.*, however, found the plastic viscosity to be unaffected by vibration (Larrard et al., 1997).

With regards to the yield stress, Tattersall *et al.* concluded that concrete under vibration loses its yield stress (Tattersall & Baker, 1988; Tattersall & Banfill, 1983). Kakuta and Kojima found that concrete under vibration changes from a thixotropic material with a yield stress to an apparently nonthixotropic shear-thinning material with little or no yield stress (Kakuta & Kojima, 1989). de Larrard *et al* found that, under vibration, the yield stress of the concrete mixtures used in their studies decreased to half its magnitude, and in some cases, became negligible (Larrard et al., 1997). L'Hermite and Touron showed that the yield stress in fresh concrete during vibration is 0.001 MPa compared with about 0.02 MPa at rest (L'Hermite & Touron, 1948). Thus, yield stress during vibration is reduced to about 5% of the value at rest.

Under vibration, flow curves obtained for concrete are below the flow curve obtained in the unvibrated state (Larrard et al., 1997), at least at low shear rates (Kakuta & Kojima, 1989; Tattersall & Baker, 1988). As show Figure 2-5, the plastic viscosity at a particular shear rate is smaller when the concrete is vibrated than for the corresponding case when the concrete is not vibrated. Therefore, the segregation tendency is expected to be higher when the concrete is subjected to vibration than when it is not.

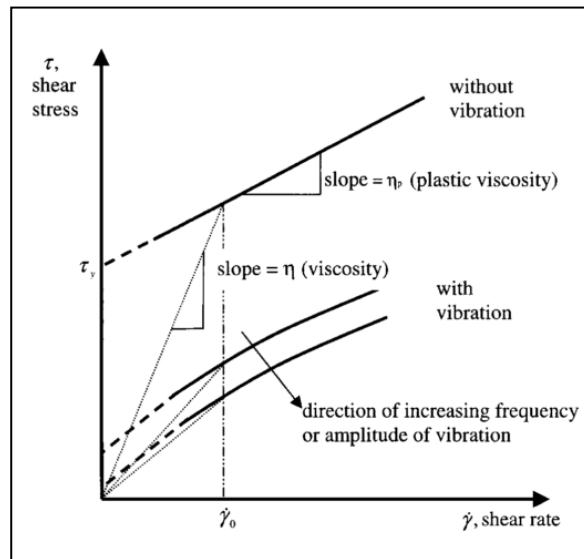


Figure 2-5: Schematic of shear stress versus strain rate curves for Bingham plastic materials (Petrou, Wan, et al., 2000)

Petrou *et al.* studied the aggregate settlement in concrete in real-time using a scintillation camera to observe and record settlement of radioactively “tagged” aggregate in mortar and concrete during vibration. They found that, prior to vibration and after the cessation of vibration, there was no noticeable aggregate settlement, as shown in Figure 2-6 (Petrou, Harries, Gadala-Maria, & Kolli, 2000).

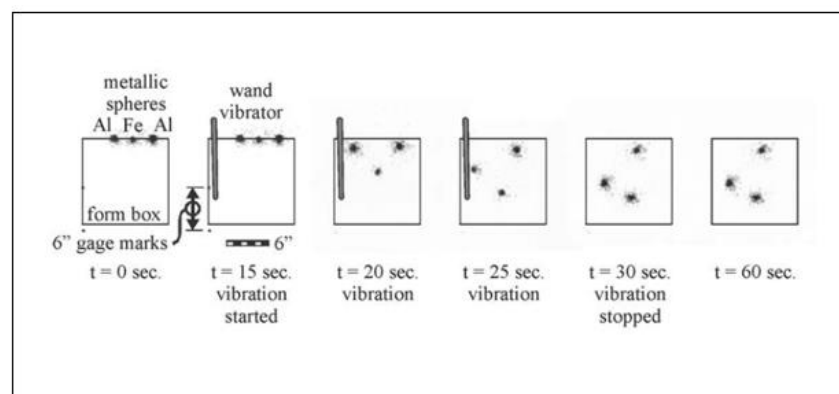


Figure 2-6: Sample results from scintillation camera experiment. (Petrou, Harries, et al., 2000)

Safawi *et al.* studied the relationship between concrete rheology and segregation of normal-weight aggregate during vibration (Safawi, Iwaki, & Miura, 2004, 2005). They estimated the yield stress and the viscosity of concrete using the slump flow test (ACI Committee 238, 2008) and the V-funnel test (Hafidi, 2013), respectively. V-funnel test consist in filled a V-shaped funnel with fresh concrete and measure the time taken for it to flow out (V-time). A high V-time indicates a high viscous condition of mixture. Figure 2-7 shows the effect on SC values of the slump flow and V-time. A higher SC value indicates a higher segregation of the mixture. From this study, the viscosity of concrete estimated from the V-funnel test is shown as being a more important parameter in segregation than flowability when considering vibration. The same results were obtained by Chia *et al.* in LWC (Chia, Kho, & Zhang, 2005).

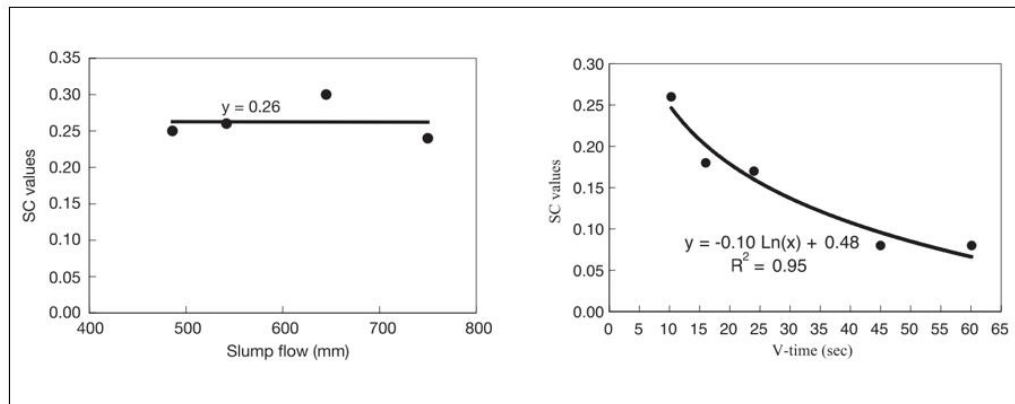


Figure 2-7: Variation between SC values with slump flow and V-time (Safawi *et al.*, 2004)

### 2.3. Coarse aggregate effect on segregation

The settling velocity of aggregates during vibration is determined by the relationship between gravitational force and drag force (Petrou, Wan, *et al.*, 2000). Higher values of gravitational force, which is determined by the volume of the aggregate and

density difference between aggregate and mortar, facilitate aggregate settlement. On the other hand, higher values of drag force, which is related to the mortar viscosity and aggregate shape, reduce aggregate settlement. Leith studied the drag force on nonspherical objects (i.e. aggregates) in viscoelastic flows (i.e. mortar) (Leith, 1987). He established that pressure on the surface of the object determined one-third of the total drag force and the other two thirds are determined by the friction drag, from the tangential shear stress at the object surface. Therefore, the settling velocity of an aggregate is more influenced by its specific surface area rather than to its size.

Previous researchers (Chia et al., 2005; B. Esmailkhanian, Khayat, Yahia, & Feys, 2014; Petrou, Harries, et al., 2000; Safawi et al., 2004, 2005; Shen, Struble, & Lange, 2009) have studied the relationship between aggregate size and shape and segregation tendency. Shen *et al.* shown that a reduction of 30% of maximum size of aggregate (MSA) greatly reduced segregation (Shen et al., 2009). The lower segregation tendency shown in mixtures with lower MSA was mainly attributed to increased drag force provided by mortar on smaller aggregates, which have a higher specific surface area. Esmailkhanian *et al.* compare segregation in concrete using either crushed aggregate or rounded aggregate with similar particle size distribution and found that the segregation tendency was not significantly different for the two mixtures. This result was explained by the fact that the aggregate surface to volume ratio does not change considerably between the two mixtures (B. Esmailkhanian et al., 2014).

Chia et al. and Petrou et al. studied the settlement of lightweight (Chia et al., 2005) and heavyweight (Petrou, Harries, et al., 2000) aggregates in concrete, respectively. Both found that concrete mixtures that present higher difference between the densities of coarse aggregate and mortar have a greater segregation tendency, which was mainly attributed to increased gravitational force.

Esmailkhanian *et al.* tested three mixtures with relative paste volume of 32%, 38% and 40%. They results shows that increasing the paste volume significantly increased

concrete segregation (Behrouz Esmailkhanian, Feys, Khayat, & Yahia, 2014). One reason for this phenomenon is that increasing the paste volume provides more interstitial space for aggregate particles to move and segregate. Other researchers showed that an increase of 20% of the aggregate volume fraction produces a reduction of 30% in the segregation tendency (Shen, Struble, & Lange, 2010).

In addition, Phillips *et al.* stated that when particle volume fraction approaches the maximum fraction, i.e. paste volume reduces; the plastic viscosity tends towards infinity making any further particle migration virtually impossible (Phillips, Armstrong, Brown, Graham, & Abbott, 1992). They showed that for a flow through a cylinder, increasing particle volume fraction decreased heterogeneities across the cylinder section, which reduce segregation.

Results obtained by previous studies (B. Esmailkhanian et al., 2014; Behrouz Esmailkhanian et al., 2014; Shen et al., 2010) showed that mixture with a more uniform grading aggregate present lower segregation tendency. As with aggregate size, the effect of aggregate gradation can also be explained by increased drag force due to higher specific surface area of the graded aggregates (Shen et al., 2010). Another possible factor is a lattice effect, whereby smaller particles slow down the movement of middle sized one, which in turn slow down the movement of larger ones (B. Esmailkhanian et al., 2014).

The relationship between aggregate properties and segregation tendency of concrete during vibration have been studied by several researchers over the last decade. However, the combined effect or interaction between coarse aggregate properties requires further investigation.

#### 2.4. Vibratory energy effect on segregation

Banfill *et al.* found that movement of fresh concrete and that of particles within the concrete (i.e. segregation) occurs when the energy input by the vibratory wave is sufficient to overcome the force of attraction between the cement particles to reduce the yield stress (P. F. G. Banfill, Xu, & Domone, 1999). The energy equation, postulated by Kirkham and White, states that (Kirkham, 1963):

$$W = c_1 \cdot m \cdot s^2 \cdot f^3 \cdot t \quad (5)$$

Where  $W$  is the energy input by the vibration;  $c_1$  is a constant, depending on stiffness and damping in concrete;  $m$  is the concrete mass;  $s$  is the amplitude of vibration;  $f$  is the frequency of vibration and  $t$  is the vibration time. The equation is a function of vibratory amplitude and frequency, which are also related to the maximum acceleration during the vibration ( $a_{max}$ ), given in Eq. 6.

$$a_{max} = 4 \cdot \pi^2 \cdot f^2 \cdot s \quad (6)$$

There is a minimum amplitude for given concrete below which vibration has no effect and the yield stress of the fresh concrete is not reduced sufficiently for movement or segregation occur (Tattersall & Baker, 1988). This is independent of vibration duration. In addition, they reported that at low shear rates, the viscosity decreases with increasing frequency and amplitude of the vibration. Therefore, aggregate settlement is expected to become more pronounced when the frequency and amplitude of vibration are increased.

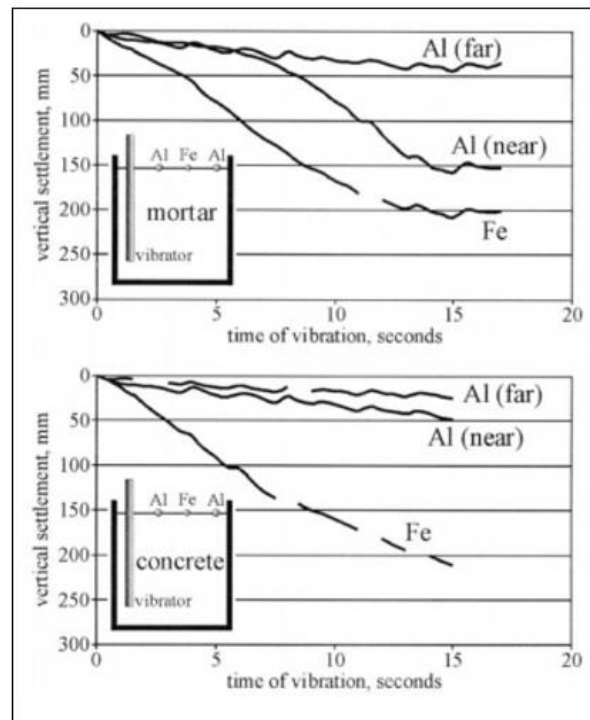


Figure 2-8: Aggregate settlement vs. time (Petrou, Harries, et al., 2000)

Previous researches study the effect of vibration time on segregation tendency (Mackechnie et al., 2007; Petrou, Harries, et al., 2000; Petrou, Wan, et al., 2000; Safawi et al., 2004, 2005). As can be seen from the slopes of the settlement curves, shown in Figure 2-8, once vibration begins, the aggregates rapidly reached their terminal velocities, which are constant during the vibration process (Petrou, Harries, et al., 2000).

Figure 2-9 shows the effect of vibration amplitude and frequency in the segregation tendency of concretes with different slump flows (Safawi et al., 2005). There was an obvious correlation between bigger amplitude and segregation tendency. Vibrators impart a vibratory force into the concrete through a combination of frequency and amplitude (ACI Committee 309, 2008). The higher the amplitude the bigger the vibratory force exerted on the concrete mass. That explains the reason for the larger segregation in bigger amplitude. On the other hand, all three frequencies tested by

Safawi *et al.* (2005) are essentially the same. Therefore, as was expected, the segregation tendency follows the same pattern to one another.

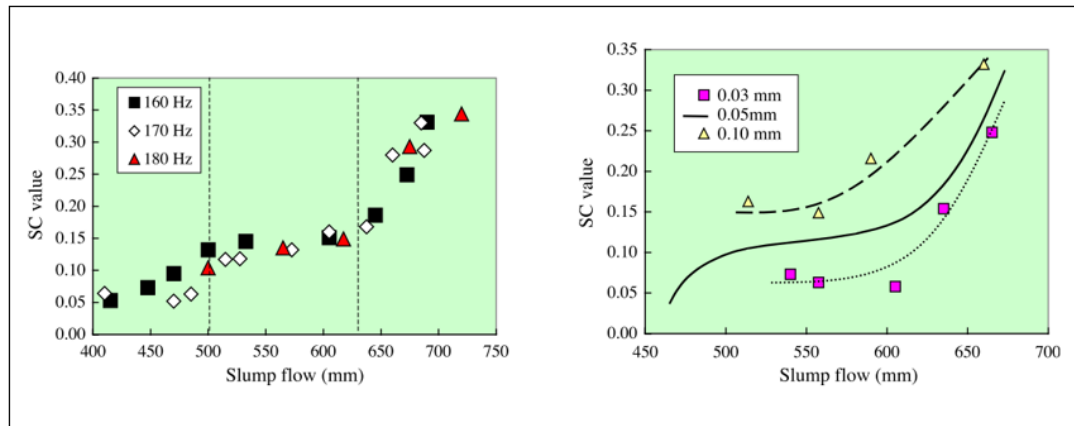


Figure 2-9: Effect of vibration amplitude and frequency in concrete segregation (Safawi *et al.*, 2005)

### **3. SUMMARY OF CONDUCTED WORK**

#### **3.1. Research Gap**

The fresh properties and mixture design of stratified concrete have been limited studied. These properties affects the segregation control, which is one of the major technical concerns of the stratified concrete. It is desired to segregate the concrete mix during compaction, but that remains homogeneous during casting. The effect in concrete segregation of aggregate properties (B. Esmaeilkhani et al., 2014; Shen et al., 2009), concrete rheology (Chia et al., 2005; Petrou, Wan, et al., 2000; Safawi et al., 2004; Seng, 2006) and vibration characteristics (Mackechnie et al., 2007; Safawi et al., 2005) have been studied separately. Nevertheless, the combined effect or interaction between these factors requires further investigation to understand the stratification process.

The use of precast panel systems offers the opportunity to control the quality of the end product to a very high degree, because the panels are supplied from specialized precasting factories and therefore cast in controlled environment. This fact is very important for stratified concrete specimens, due to the vibration process must be controlled to achieve a correct stratification. However, when the panel is lifted, its dead weight induces flexural stresses that may exceed in-place construction values. Stratified concrete fresh and hardened properties have been studied at the material level (Grange, 2012; Mackechnie et al., 2009, 2007; Mackechnie & Saevarsdottir, 2007); however, neither full-scale specimens nor structural behavior in steel reinforced specimens have been studied yet.

## **3.2. Hypotheses**

The formulated hypotheses are going to be addressed in the articles presented in Chapter Four, Chapter Five and Chapter Six. Hypothesis 1 corresponds to Chapter Four. Hypothesis 2 corresponds to Chapter Five. Finally, Hypothesis 3 corresponds to Chapter Six.

### **3.2.1. Hypothesis 1**

The segregation of concrete during vibration is more related to the combined effect of coarse aggregate specific surface area and density difference between coarse aggregate and mortar rather than to each individual factor.

### **3.2.2. Hypothesis 2**

The segregation of concrete during vibration can be mainly explained by the combined effect of mortar viscosity, density difference between mortar and coarse aggregate, specific surface area of coarse aggregate and energy applied by mass of concrete.

### **3.2.3. Hypothesis 3**

Stratified concrete presents a normal behavior under flexure loads; therefore this novel material does not need special design and analysis procedures.

### 3.3. Objectives

The main objectives is to understand the combined effect of mixture design parameters and vibration characteristics on concrete segregation and the assessment of flexural behavior, design and analysis of reinforced stratified concrete specimens.

The specific objectives are:

- i) Evaluate the independent effect of aggregate parameters (density difference between mortar and coarse aggregate and specific surface area of coarse aggregate) in the segregation of concrete during vibration.
- ii) Evaluate the combined effect of aggregate parameters (density difference between mortar and coarse aggregate and volume-to-surface area ratio of coarse aggregate) in the segregation of concrete during vibration.
- iii) Evaluate the effect of vibratory energy in the segregation of concrete.
- iv) Evaluate the effect of mortar viscosity in the segregation of concrete during vibration.
- v) Evaluate the combined effect of mixture design factors (density difference between mortar and coarse aggregate, specific surface area of coarse aggregate and mortar viscosity) and vibratory energy in the segregation of concrete.
- vi) Characterize the flexural behavior of reinforced stratified concrete specimens.
- vii) Propose an analytical modelling that relates the mechanical properties of stratified concrete layers to the flexural behavior of reinforced stratified concrete specimens.

viii) Evaluate the use of rectangular stress-block method on flexural design of reinforced stratified concrete specimens.

### **3.4. Methodology**

A literature review was conducted to analyze the state of the art of stratified concrete hardened and fresh properties and the effect of mixture design factors and vibration characteristics in the segregation of concrete. The methods to quantify the segregation of concrete and the current experimental procedures for physical and mechanical properties of unreinforced and reinforced concrete samples were also studied. The materials were selected based on the literature results and their availability in Chile. The experimental program was designed in order to assess the objectives proposed. The experimental program consisted in three phases. 14 concrete mixtures were used at phases one and two (Chapter Four, and Chapter Five) where their segregation and physical properties were measured, and 2 concrete mixtures were used at last phase (Chapter Six) where their physical and mechanical properties were measured. Multiple linear regression models for segregation were assessed to evaluate the impact of studied mixture design factors and vibration characteristics. Fiber element analytical model for flexural behavior of reinforced stratified concrete specimens were also investigated to evaluate the effect of the concrete layers properties. The conclusions were obtained from the analysis of the results.

#### 4. UNDERSTANDING THE RELATIONSHIP BETWEEN THE STABILITY OF CONCRETE UNDER VIBRATION AND COARSE AGGREGATE DENSITY AND SIZE

Ivan Navarrete <sup>a</sup>, Mauricio Lopez <sup>a,b,c</sup>

<sup>a</sup> Department of Construction Engineering and Management, School of Engineering, Pontificia Universidad Catolica de Chile, Santiago, Chile

<sup>b</sup> Center for Sustainable Urban development (CEDEUS), Pontificia Universidad Catolica de Chile, Vicuña Mackenna 4860, Casilla 306, Correo 22, Santiago, Chile

<sup>c</sup> Research Center for Nanotechnology and Advanced Materials “CIEN-UC”, Pontificia Universidad Catolica de Chile, Santiago, Chile

##### **Abstract**

Segregation of aggregate, which ultimately determines the strength and durability of concrete, is one of the major problems during construction. Three factors and their effects on the stability of fresh concrete under vibration were studied. Based on the statistical analysis of the experimental results, it was concluded that the observed rate of segregation is an intrinsic property of concrete and is independent of the vibration time applied. The segregation tendency of a concrete mixture is mainly explained by the interaction between the specific surface of coarse aggregate and the difference in density between the aggregate and mortar phase rather than by each individual factor independently.

##### **Keywords**

Fresh concrete, vibration, aggregate size, aggregate density, segregation rate, image analysis.

#### 4.1. Introduction

Segregation, the tendency for coarse aggregate to separate from mortar, remains one of the major problems in fresh concrete. The consequences of segregation are numerous and may affect the strength and durability of structures (ACI Committee 238, 2008). However, the construction workforce is mainly unskilled (Finger, González, & Kern, 2015). Thus, control of the mixture design is necessary to assess a good final quality of the construction.

The rheology of fresh concrete is complex owing to its multi-composition and the changes in properties upon hydration. Previous researchers (Tattersall & Banfill, 1983) have shown that the flow behavior of fresh concrete can be reasonably approximated by the Bingham model:

$$\tau = \tau_0 + \eta_p \cdot \dot{\gamma} \quad (1)$$

Where  $\tau$  is the shear stress,  $\tau_0$  is the yield stress,  $\eta_p$  is the plastic viscosity, and  $\dot{\gamma}$  is the shear rate. Therefore, the flow of concrete can be described by two parameters: yield stress and plastic viscosity.

Fresh concrete may be considered as a two-phase composite material with coarse aggregate particles in a mortar matrix. The settlement of a particle in a fluid with Bingham plastic behavior has been predicted by Beris et al. (Beris et al., 1985). They concluded that a sphere will settle when the yield stress parameter ( $Y_g$ ), defined in Eq. 2, is less than 0.143, assuming that the particle density is higher than that of the fluid.

$$Y_g = \frac{3 \cdot \tau_0}{2 \cdot R \cdot |\Delta \rho| \cdot g} \quad (2)$$

Where  $|\Delta\rho|$  is the density difference between the particle and the fluid,  $R$  is the radius of the particle,  $\tau_0$  is the yield stress of the fluid, and  $g$  is the gravitational acceleration. Thus, in fresh concrete, the beginning of coarse aggregate settlement is related to the yield stress of the mortar, the density difference between coarse aggregate and mortar, and the size of the coarse aggregate. Once the settlement starts, a spherical particle will sink into the Bingham fluid with a velocity  $U$ , which may be derived from Stoke's drag equation (Petrou, Harries, et al., 2000):

$$U = \frac{2}{9} \cdot \frac{R^2 \cdot |\Delta\rho| \cdot g}{\eta_p \cdot C_s} \quad (3)$$

Where  $\eta_p$  is the plastic viscosity of the fluid, and  $C_s$  is Stoke's drag coefficient. Therefore, the velocity of the aggregate settlement is directly dependent on the difference in density between the coarse aggregate and the mortar and the size of coarse aggregate, and it is inversely dependent on the plastic viscosity and drag coefficient. When the aggregates' density is lower than that of the mortar, the principal parameters that affect the stability of the fresh concrete are the same; i.e., equation 3 is still valid and predicts an upward movement of coarse aggregate (Chia et al., 2005).

Tattersall and Baker (Tattersall & Baker, 1988) showed that when vibration is applied, there is a significant reduction in the yield stress and a decrease in the viscosity of the concrete. However, de Larrard et al. (Larrard et al., 1997) found that the plastic viscosity is unaffected by vibration, which is consistent with previous research (Chia et al., 2005; Petrou, Wan, et al., 2000; Safawi et al., 2005) that found that concrete viscosity is more important than yield stress for concrete segregation during vibration.

Petrou et al. (Petrou, Harries, et al., 2000) studied the aggregate settlement in concrete in real time using a scintillation camera to observe and record the settlement

of radioactively “tagged” aggregate in mortar and concrete during vibration. They found a linear relationship between aggregate settlement and vibration time.

Chia et al. (Chia et al., 2005) and Petrou et al. (Petrou, Harries, et al., 2000) studied the settlement of lightweight and heavyweight aggregates in concrete, respectively. Both found that concrete mixtures that present a higher difference between the densities of coarse aggregate and mortar have a greater segregation tendency.

Previous researchers (Chia et al., 2005; B. Esmailkhanian et al., 2014; Petrou, Harries, et al., 2000; Shen et al., 2009) have studied the relationship between aggregate size and shape and segregation tendency. Shen et al. (Shen et al., 2009) showed that a reduction of 30% in the maximum size of aggregate (MSA) greatly reduces segregation. The lower segregation tendency shown in mixtures with lower MSA was mainly attributed to the increased drag force provided by mortar on smaller aggregates, which have a higher specific surface (i.e., surface area-to-volume ratio). In contrast, Esmailkhanian et al. (B. Esmailkhanian et al., 2014) compared segregation in concrete using either crushed aggregate or rounded aggregate with similar particle size distribution and found that the segregation tendency was not significantly different between the two mixtures. This result was explained by the fact that the aggregate surface-to-volume ratio does not change considerably between the two mixtures.

The relationship between the aggregate properties and segregation tendency of concrete during vibration has been studied by several researchers over the last decade. However, the combined effect or interaction between coarse aggregate properties requires further investigation.

## **4.2. Research Significance**

The stability of fresh concrete without segregation is an important issue to be considered for concrete mixture design. The aim of this research is to assess the combined effects of coarse aggregate size and shape and the difference in density between coarse aggregate and mortar on the stability of fresh concrete under vibration. This will provide a more adequate understanding and estimate of the intrinsic segregation tendency of a concrete mixture.

## **4.3. Materials and Methods**

### **4.3.1. Materials properties and mixture proportion**

Ordinary Portland cement (OPC) with a specific gravity of 3.14 and Blaine fineness of 410 m<sup>2</sup>/kg was used, and a natural river sand with a fineness modulus of 3.18 was used as fine aggregate (FA) for all mixtures. The absorption of FA was 0.97%, and the specific gravity was 2.72 at the saturated surface dry (SSD) condition. Additionally, high-range water reducer admixture (HRWA) was used in a dosage of 0.25% by cement weight for all mixtures.

A normal-weight aggregate (NWA)—namely, gravel—and three lightweight aggregates (LWA)—namely, expanded shale, expanded clay and expanded polystyrene—were used as coarse aggregate (CA). The four types of CAs were sieved to obtain different single-sized aggregates. The physical properties of single-sized NWA and LWA used in the study are given in Table 4-1. The absorption of LWA was obtained after 72 h immersion to maximize the pore saturation (ASTM, 2013).

The aggregate specific surface area (SSA) of CA was measured on concrete samples by means of stereology parameters. The estimation of SSA was made from vertical

uniform random (VUR) sections using an unbiased stereology technique based on cycloids. Cycloids were used because they are considered to be isotropic lines on VUR sections in 3D space (Mouton, 2002a). SSA is estimated from Eq. 4.

$$S_v = 2 \cdot \frac{\sum I}{\sum P \cdot l} \cdot \frac{V_c}{V_a} \quad (4)$$

Where  $\sum I$  is the number of intersections;  $\sum P$  is the number of points counted;  $l$  is the length of one test line;  $V_c$  is the volume of concrete of the sample and  $V_a$  is the volume of aggregate of the sample.

Table 4-1: Physical properties of single-sized aggregates

Aggregate	Size (mm)	SSA (1/mm)	SSD Density (kg/m <sup>3</sup> )	Absorption, 72 hr (%)
Gravel	19.0 – 25.4	0.69	2600	2.44
	12.7 – 19.0	0.97	2630	1.74
	9.5 – 12.7	1.59	2710	1.29
	4.8 – 9.5	1.74	2720	0.99
Expanded Shale	12.7 – 19.0	0.90	1370	12.47
	9.5 – 12.7	1.47	1410	12.21
	4.8 – 9.5	1.76	1470	12.01
Expanded Clay	9.5 – 12.7	1.38	950	22.72
	4.8 – 9.5	2.02	980	21.48
	2.4 – 4.8	2.72	1070	20.76
Expanded Polystyrene	4.8 – 9.5	1.98	15	-
	2.4 – 4.8	2.48	15	-

In this study, two series of concrete mixtures were prepared. Series I consisted of ten mixtures used to assess the relationship between the segregation of concrete under vibration and coarse aggregate size and the difference in density between coarse

aggregate and mortar. Series II consisted of two additional mixtures used to validate the findings and the relationship established with the concretes of Series I. The concrete mixtures had a water–cement ratio (W/C) of 0.45 and consisted of approximately 70% mortar and 30% coarse aggregate by volume; the proportion of each constituent was kept constant in all mixtures. Table 4-2 presents the mixture proportions of both series. The moisture states of FA and CA in the given mixture proportions were SSD.

Table 4-2: Concrete mixture proportions

	Mixture ID	OPC (kg/m <sup>3</sup> )	Water (kg/m <sup>3</sup> )	FA (kg/m <sup>3</sup> )	CA (kg/m <sup>3</sup> )	HRWA (kg/m <sup>3</sup> )	CA type	CA size (mm)
Series I	G-1	440	200	950	780	1.1	Gravel	19.0
	G-2	440	200	950	789	1.1	Gravel	12.7
	ES-1	440	200	950	411	1.1	Exp. Shale	12.7
	ES-2	440	200	950	423	1.1	Exp. Shale	9.5
	ES-3	440	200	950	441	1.1	Exp. Shale	4.8
	EC-1	440	200	950	285	1.1	Exp. Clay	9.5
	EC-2	440	200	950	294	1.1	Exp. Clay	4.8
	EC-3	440	200	950	321	1.1	Exp. Clay	2.4
	EP-1	440	200	950	4.5	1.1	Exp. Pol.	4.8
	EP-2	440	200	950	4.5	1.1	Exp. Pol.	2.4
Series II	G-3	440	200	950	813	1.1	Gravel	9.5
	G-4	440	200	950	816	1.1	Gravel	4.80

#### 4.3.2. Segregation measurement

Mouton (Mouton, 2002a) showed that the area of an object on random surfaces cut through the reference space is proportional to the 3D volume of the object in the reference space. Shen *et al.* (Shen et al., 2009) and Kwasny *et al.* (Kwasny, Asce, Sonebi, Taylor, et al., 2012) showed that estimating area by pixel counting is an adequate method to quantify aggregate distribution in concrete samples. Additionally, Gundersen *et al.* (Gundersen, Jensen, Kiêu, & Nielsen, 1999) showed

that point counting is an efficient alternative to estimating area by pixel counting. Therefore, the estimation of aggregate volume fraction at different heights was made with an unbiased stereology technique based on count pointing.

Fifteen 10 cm × 20 cm cylinders were cast for each mixture and were vibrated for different vibration times of 0, 30, 60, 90 and 120 s. The vibration table used had a fixed frequency of 50 Hz, and the maximum acceleration measured during vibration was 12 g. At the age of 2 days, the concrete specimens were saw-cut through the longitudinal axis, washed from dust, and air-dried in the laboratory. The dry-cut surfaces were photographed and used to measure the distribution of coarse aggregate.

The photographs of the tested specimens were divided into three equal sections (top, middle and bottom). For the top and bottom sections, the volume of coarse aggregate was calculated by using the following equation:

$$V_{ai} = \frac{P_{ai}}{P_{refi}} \cdot 100\% \quad (5)$$

where  $P_{ai}$  is the sum of the points reaching the aggregate in section i,  $P_{refi}$  is the sum of the points reaching section i, and  $V_{ai}$  is the aggregate volume fraction of section i.

To evaluate segregation, the volumetric index (VI), proposed by Esmailkhanian *et al.* (Behrouz Esmailkhanian et al., 2014), was calculated:

$$VI (\%) = 2 \cdot \frac{|V_{at} - V_{ab}|}{V_{at} + V_{ab}} \cdot 100\% \quad (6)$$

Where  $V_{at}$  and  $V_{ab}$  are the aggregate volume fractions of the top and bottom sections, respectively.

#### 4.4. Results and Discussions

##### 4.4.1. Preliminary Mortar Characterization

Table 4-3 lists the mixture proportions and physical properties of the mortar used (M1). The rheological behavior of the mortars is determined by the W/C ratio and the ratio of sand to mortar (s/m) (Singh, Munjal, & Thammishetti, 2015). Previous researchers established procedures for computing normal-weight (Mehta & Monteiro, 2014) and lightweight (Chandra & Berntsson, 2003) concrete. According to these procedures, the ratio of s/m and the ratio of W/C of M1 are similar to those of conventional mortars.

Table 4-3: Mortar mixture proportioning

Sample ID	Water (kg/m <sup>3</sup> )	Cement (kg/m <sup>3</sup> )	Sand (kg/m <sup>3</sup> )	HRWA (kg/m <sup>3</sup> )	W/C	s/m	Density (Ton/m <sup>3</sup> )
M1	291	635	1376	1.58	0.46	0.60	2.31

Several authors (Petrou, Harries, et al., 2000; Petrou, Wan, et al., 2000; Safawi et al., 2004, 2005) have shown that the segregation tendency of concrete is related to its mortar viscosity and has no relation to its mortar yield stress. However, Hafidi *et al.* (Hafidi, 2013) established that a direct relation exists between the mortar viscosity and its V-funnel flow time (V-time) (ACI Committee 238, 2008). Therefore, the V-funnel test was used to characterize the rheological behavior of M1, which showed a V-time of 6.8 s. This result is similar to the V-times reported by Safawi *et al.* (Safawi et al., 2005) for mixtures of conventional mortars.

#### 4.4.2. Limit for acceptable volumetric index

Esmailkhanian *et al.* (B. Esmailkhanian et al., 2014) measured the segregation of self-consolidating concrete and established that a VI of 25% can be considered as a limit for acceptable segregation resistance. In contrast, Kwasny et al. (Kwasny, Asce, Sonebi, Taylor, et al., 2012) studied the stability of semi-lightweight concrete and proposed that a concrete can be considered to be segregated when the variation of aggregate content between the bottom and top sections exceeds 20%.

Figure 4-1 shows the tested specimens of mixtures EC-3 (Figure 4-1.a), EP-2 (Figure 4-1.b) and G-1 (Figure 4-1.c), which were vibrated for 30 s and present VI values lower than 20%. Figure 4-2. shows tested specimens of the same mixtures shown in Figure 4-1. that were vibrated for 60 s and present VI values higher than 30%. It can be observed that specimens with VI values lower than 20% did not present segregation, and specimens with VI values higher than 30% presented segregation. Therefore, a conservative VI value of 20% can be considered a limit for acceptable segregation.

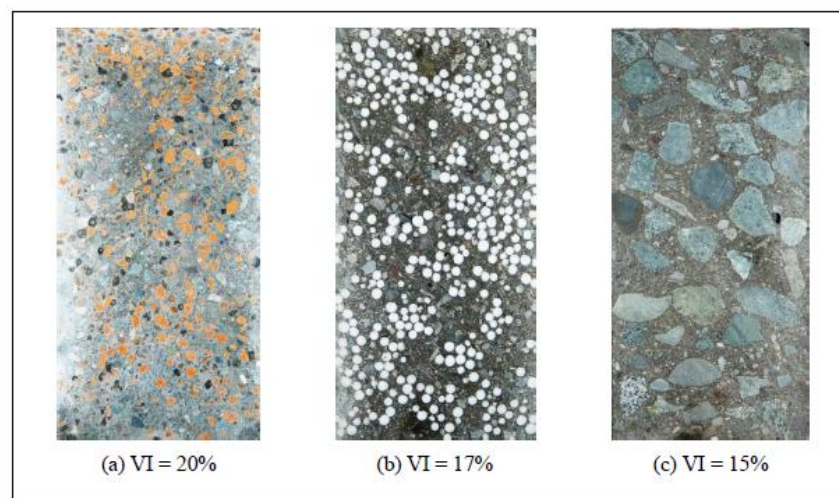


Figure 4-1: Test specimens with a VI lower than 20%

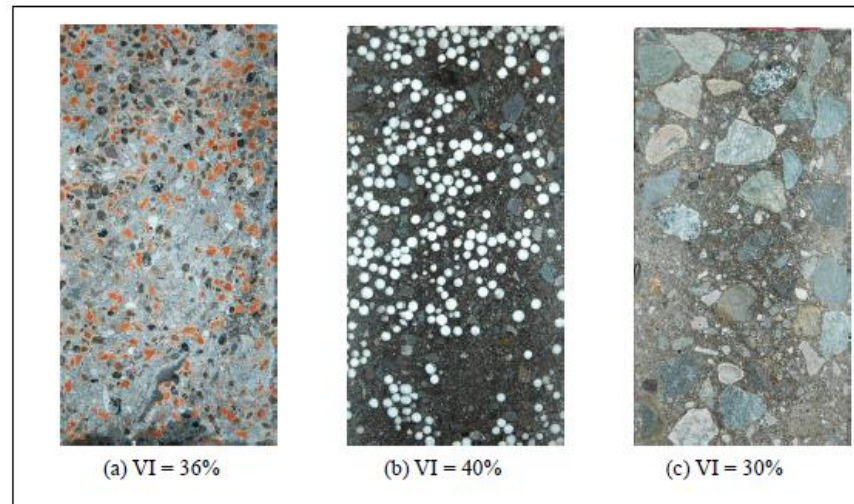


Figure 4-2: Test specimens with a VI higher than 30%

Previous studies (Petrou, Harries, et al., 2000; Petrou, Wan, et al., 2000) showed that without vibration, typically sized aggregate does not settle in mortars with similar V-times to M1. Furthermore, settlement stops immediately after vibration is terminated. Table 4-4 shows that when no vibration is applied, all the tested mixtures present a VI value lower than 7.0%, which is similar to the results shown by Chia (Chia et al., 2005) in non-segregated concretes. Therefore, as expected, no static segregation occurred in the tested mixtures. Accordingly, it can be stated that the segregation presented on tested specimens was only due to the segregation produced by vibration.

#### 4.4.3. Segregation rate

Aggregate parameters and VI average values for each Series I mixture and vibration time are summarized in Table 4-4. The equivalent specific surface area radius ( $R_{SSA}$ ) in Table 4-4 was calculated by using the following equation:

$$R_{SSA} = \frac{3}{SSA} \quad (7)$$

where SSA is the specific surface area of the aggregate. This value represents the ratio between the volume and the surface area of the aggregate used on each mixture. The density difference between aggregate and mortar ( $|\Delta\rho|$ ) in Table 4-4 was calculated as the absolute value of the difference between SSD density of the aggregate and the density of freshmortar.

Table 4-4: Aggregate parameters and stratification coefficients of series I concrete mixtures

Sample ID	Size (mm)	R <sub>SSA</sub> (mm)	$ \Delta\rho $ (Ton/m <sup>3</sup> )	VI (%)				
				0 s	30 s	60 s	90 s	120 s
G-1	19.05	4.35	0.42	1	33	55.8	84.9	100.5
G-2	12.7	3.10	0.42	0.5	8.4	27.2	34.6	49.5
ES-1	12.7	3.34	0.89	7	70.4	133.3	154.4	183.1
ES-2	9.53	2.04	0.85	2.1	11	17.3	55.4	85.1
ES-3	6.35	1.71	0.79	1.9	10.3	21.2	32.3	61.7
EC-1	9.53	2.17	1.31	5.3	50.1	96.6	150.4	186.6
EC-2	6.35	1.48	1.28	1.5	14.1	41.4	78.7	103.3
EC-3	3.18	1.10	1.19	2.3	9.4	20.1	25.2	37.9
EP-1	6.35	1.52	2.25	6.5	78.7	155.8	187.8	200
EP-2	3.18	1.21	2.25	4.1	40.3	129.4	152.1	186.6

A multiple linear regression (MLR) model that relates VI values with the parameters shown in Table 4-4 was used to assess the relation between VI values and vibration time. The four parameters explained 80% of the variability of the VI value, and each one presented a level of significance below 0.05. Moreover, an MLR model that relates segregation rate ( $U_t$ ), calculated as the ratio between VI value and vibration time with the parameters shown in Table 4-4, was used to assess the relation between segregation rate and vibration time. The four parameters explained 77% of the variability of the segregation rate, and only the vibration time is insignificant with a

P-value of 0.45. Therefore, a linear relation exists between vibration time and VI values.

Furthermore, it can be stated that the segregation rate is an intrinsic property of the concrete and is independent of the vibration time applied. This is in accordance with the results presented by Petrou (Petrou, Harries, et al., 2000), who showed that aggregate settling velocity in mortar is constant during the vibration process. Therefore, the segregation rates of each mixture, summarized in Table 4-5, are preferred instead of VI values to analyze the effect of the studied aggregate properties on concrete segregation.

Table 4-5: Segregation rate of concrete mixtures

Sample ID	Ut (%/s)				Average
	30 s	60 s	90 s	120 s	
G-1	1.1	0.93	0.94	0.84	0.95
G-2	0.28	0.46	0.38	0.41	0.38
S-1	2.35	2.22	1.71	1.52	1.95
S-2	0.37	0.29	0.61	0.71	0.50
S-3	0.34	0.35	0.35	0.51	0.39
EC-1	1.67	1.61	1.67	1.56	1.63
EC-2	0.47	0.69	0.87	0.86	0.72
EC-3	0.31	0.33	0.28	0.32	0.31
EP-1	2.62	3.1	2.14	1.66	2.38
EP-2	1.34	2.15	1.69	1.55	1.68

#### 4.4.4. $R_{SSA}$ value vs aggregate size

The settling velocity of aggregates during vibration is determined by the relationship between gravitational force and drag force (Petrou, Wan, et al., 2000). Higher values

of gravitational force, which is determined by the volume of the aggregate and  $|\Delta\rho|$  value, facilitate aggregate settlement. Conversely, higher values of drag force, which is related to the mortar viscosity and aggregate shape, reduce aggregate settlement. Leith (Leith, 1987) studied the drag force on nonspherical objects (i.e., aggregates) in viscoelastic flows (i.e., mortar). He established that pressure on the surface of the object determined one-third of the total drag force and that the other two-thirds are determined by the friction drag from the tangential shear stress at the object surface. Therefore, the settling velocity of an aggregate is influenced more by its  $R_{SSA}$  value than by its size.

Two MLR models were developed for the segregation rate; in the first one, the independent variables were  $R_{SSA}$  and  $|\Delta\rho|$ , which explained 76% of the variability of the segregation rate. In the second model, the independent variables were the aggregate size and  $|\Delta\rho|$ , which explained 71% of the variability of the segregation rate. Therefore, the segregation rate variability is better explained by  $R_{SSA}$  than by the aggregate size.

#### 4.4.5. Linear regression model for segregation rate

MLR models were proposed to correlate the segregation rate with  $R_{SSA}$  and  $|\Delta\rho|$ . The first proposed model was similar to the model used in section 4.4.4, which is represented in Eq. 8.

$$U_{t.est} = \alpha_0 + \alpha_1 \cdot R_{SSA} + \alpha_2 \cdot |\Delta\rho| \quad (8)$$

where  $U_{t.est}$  is the estimated segregation rate in %/s,  $R_{SSA}$  is in mm, and  $|\Delta\rho|$  is in  $\text{ton/m}^3$ . Additionally,  $\alpha_i$  includes the MLR coefficients ( $i = 0,1,2$ ).

Table 4-6 presents the first proposed model summary and coefficient results. The  $\alpha_0$ ,  $\alpha_1$  and  $\alpha_2$  values are shown in Table 4-6. These values represent the individual

contribution of each parameter on the segregation rate of concrete for a level of significance of 0.05. With this model,  $R_{SSA}$  and  $|\Delta_p|$  explained 76% of the variability of the segregation rate of the concrete.

Table 4-6: First proposed model summary and coefficient results of the segregation rate regression analysis

	Coefficients	Standard Error	T Statistic	P-value	95% C.I. ( $\pm$ )
$\alpha_0$	-2.01	0.32	- 6.28	0.00	0.65
$\alpha_1$	0.63	0.08	7.56	0.00	0.17
$\alpha_2$	1.47	0.14	10.79	0.00	0.28

$R^2=0.76$

Figure 4-3 shows the relationship between the segregation rate and the aggregate  $R_{SSA}$  value of each concrete mixture. The corresponding  $|\Delta_p|$  value, in  $\text{ton/m}^3$ , is shown next to each data series. From Figure 4-3, it is observed that the segregation rate was less affected by  $R_{SSA}$  in mixtures with lower  $|\Delta_p|$  values. The relationship between the segregation rate and  $|\Delta_p|$  of each concrete mixture is shown in Figure 4-4. The corresponding  $R_{SSA}$  value, in mm, is shown next to each data series. Figure 4-4 shows that the segregation rate is more affected by  $|\Delta_p|$  in concrete mixtures that present higher  $R_{SSA}$  values. Therefore, it can be concluded that there is a correlation between  $R_{SSA}$  and  $|\Delta_p|$  on the segregation rate of concrete. This is supported by the work of Shen *et al.* (Shen et al., 2009) and Esmailkhanian *et al.* (B. Esmailkhanian et al., 2014), which showed that segregation is directly related to the aggregate mass-to-surface area ratio, which is related to the multiplication of  $|\Delta_p|$  and  $R_{SSA}$ .

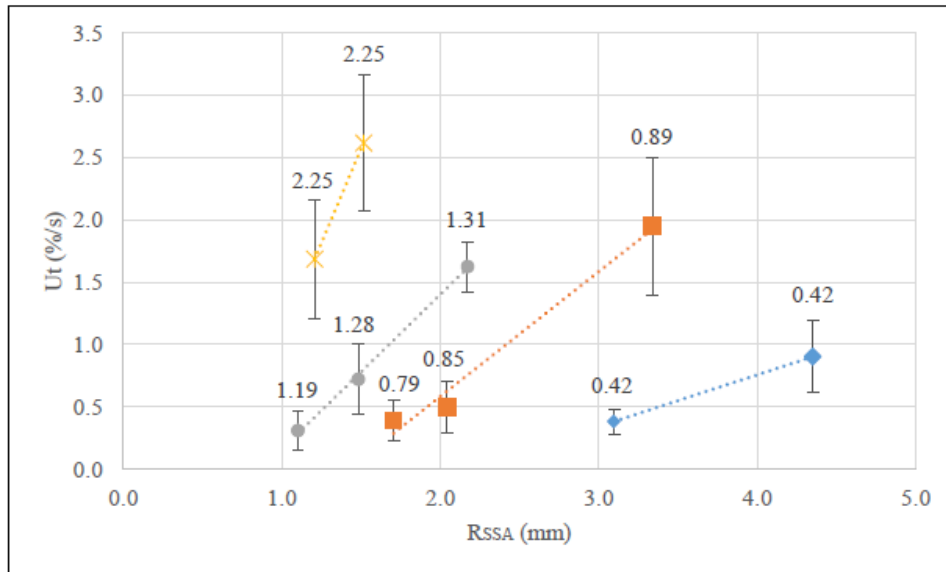


Figure 4-3: Effect of  $R_{SSA}$  value on segregation rate. (Values besides corresponding data point are  $|\Delta\rho|$  values in  $\text{Ton/m}^3$ .)

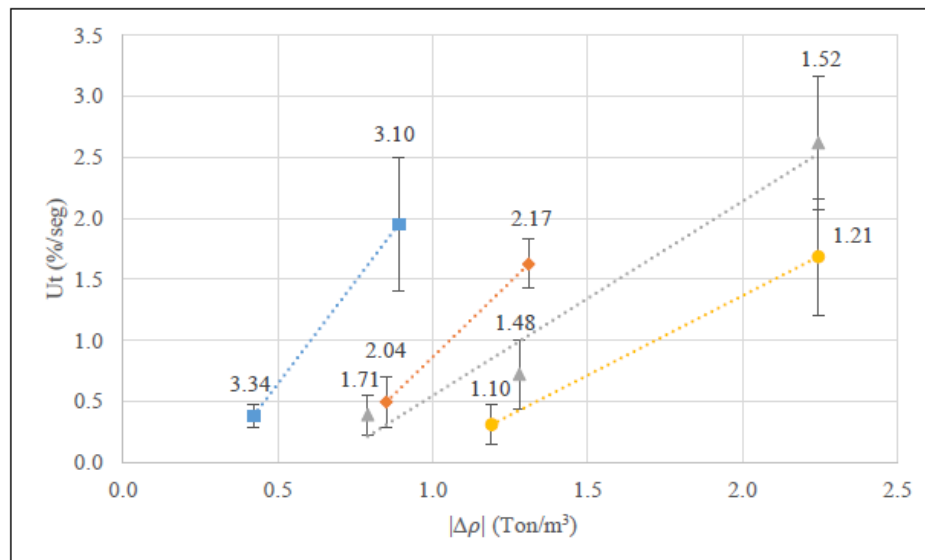


Figure 4-4: Effect of  $|\Delta\rho|$  value on segregation rate. (Values besides corresponding data points are  $R_{SSA}$  value in mm.)

Therefore, the correlation between  $|\Delta_p|$  and  $R_{SSA}$  can be represented by the product between the variables in an improved MLR model, as shown in Eq. 9.

$$U_{t,est} = \beta_0 + \beta_1 \cdot R_{SSA} + \beta_2 \cdot |\Delta_p| + \beta_3 \cdot R_{SSA} \cdot |\Delta_p| \quad (9)$$

The second model explained 89% of the variability of the segregation rate, meaning that the inclusion of the product between  $R_{SSA}$  and  $|\Delta_p|$  is significant. However, Table 4-7 shows that  $R_{SSA}$  and  $|\Delta_p|$  are not significant anymore with P-values of 0.09 and 0.16, respectively.

Table 4-7: Second proposed model summary and coefficient results of the segregation rate regression analysis.

	Coefficients	Standard Error	T Statistic	P-value	95% C.I. ( $\pm$ )
$\beta_0$	-1.37	0.24	-5.47	0.00	0.49
$\beta_1$	0.16	0.09	1.79	0.09	0.19
$\beta_2$	0.30	0.21	1.44	0.16	0.42
$\beta_3$	0.81	0.12	6.48	0.00	0.25

$R^2=0.89$

Therefore, a third model was proposed, using only the product between  $R_{SSA}$  and  $|\Delta_p|$  shown in Eq. 10.

$$U_{t,est} = \gamma_0 + \gamma_1 \cdot R_{SSA} \cdot |\Delta_p| \quad (10)$$

Table 4-8 shows that an increase in the  $R_{SSA} \cdot |\Delta_p|$  coefficient also increased the segregation rate of concrete for a level of significance below 0.05. The  $R_{SSA} \cdot |\Delta_p|$  value explained 88% of the variability of the segregation rate of concrete, which indicates a good prediction of the segregation from the linear regression model.

However, the model obtained is valid only for mixtures with similar mortar viscosities and volumes of aggregate used in this model. However, the model obtained is valid only for mixtures with similar mortar viscosities and volumes of aggregate used in this study.

Table 4-8: Third proposed model summary and coefficient results of the segregation rate regression analysis

	Coefficients	Standard Error	T Statistic	P-value	95% C.I. ( $\pm$ )
$\gamma_0$	-0.96	0.13	-7.35	0.00	0.27
$\gamma_1$	0.96	0.06	16.58	0.00	0.12

$R^2=0.88$

#### 4.4.6. Validation of the linear regression modelling of segregation rate

When comparing the model estimates of segregation rate using Eq. 10 with the experimental results (Figure 4-5), it is observed that the model shows a threshold of  $R_{SSA} \cdot |\Delta\rho|$  under which there is no segregation. For the concrete tested in this study, that threshold was 1.0 ( $\text{Ton} \cdot \text{mm}/\text{m}^3$ ). This is consistent with the findings of Beris *et al.* (Beris et al., 1985), which predicted that a spherical particle would settle in a fluid with Bingham plastic behavior only when the yield stress parameter is less than 0.143. Therefore, lower values of  $R_{SSA} \cdot |\Delta\rho|$  imply higher values of the yield stress parameter, which reduces chances for aggregate settlement.

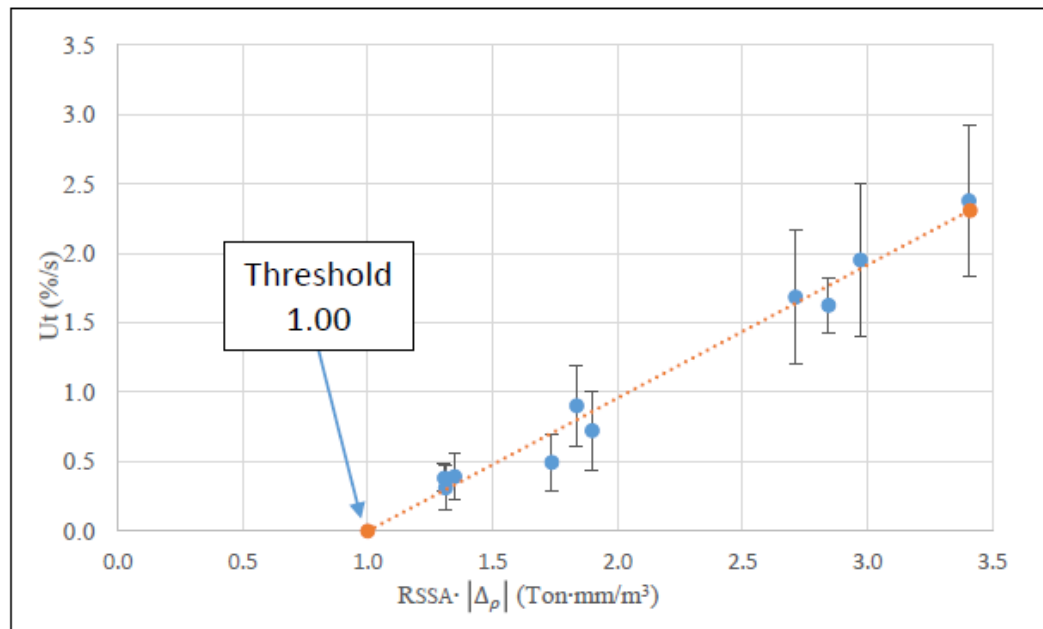


Figure 4-5: Linear regression modelling and experimental results of segregation rate

Two new concrete mixtures (Series II) that present  $R_{SSA} \cdot |\Delta\rho|$  lower than 1.00 ( $\text{Ton} \cdot \text{mm}/\text{m}^3$ ) were tested to check the proposed model. Table 4-9 shows that the VI values for the four vibration times applied were lower than 5% in both tested mixtures, which means that no segregation occurred in these mixtures, as predicted by the proposed model.

Table 4-9: Aggregate parameters and stratification coefficients of series II concrete mixtures

Sample ID	$R_{SSA}$ (mm)	$ \Delta\rho $ ( $\text{Ton}/\text{m}^3$ )	$R_{SSA} \cdot  \Delta\rho $ ( $\text{Ton} \cdot \text{mm}/\text{m}^3$ )	VI (%)			
				30 s	60 s	90 s	120 s
G-3	2.00	0.42	0.84	0.7	3.6	1.0	4.2
G-4	1.70	0.42	0.71	3.7	0.5	0.8	4.5

#### 4.5. Conclusions

This research aimed to understand the main intrinsic factors explaining segregation in concrete under vibration by investigating the combined effect of aggregate size and density difference between coarse aggregate and mortar. Twelve mixtures with four different aggregate densities and MSA were investigated. The main conclusions follow:

- (1) A volumetric index of 20% is proposed as a conservative limit for acceptable segregation in concrete. The concrete mixtures analyzed here presented a threshold below which no segregation was observed. This means that segregation can be prevented or reduced by the mixture design of concrete.
- (2) The segregation rate produced during vibration was shown to be independent of the time of vibration, so it is an intrinsic fresh property of the concrete mixture and can be used to characterize its behavior under vibration.
- (3) The volume-to-surface area ratio of coarse aggregate explained the segregation rate of concrete more precisely than MSA, meaning that the shape of the aggregate plays a significant role in segregation. That is, segregation can be reduced by either reducing MSA or increasing the angularity of coarse aggregate.
- (4) As the density difference between coarse aggregate and mortar increases, the volume-to-surface area ratio becomes more significant in explaining the segregation rate. This is relevant when using lightweight and heavyweight aggregates in normal weight mortars and implies that MSA and the shape of the coarse aggregate must be especially considered for minimizing or eliminating segregation.
- (5) The segregation tendency of a concrete mixture is more related to the combined effect of its volume-to-surface ratio and density difference between coarse aggregate and mortar than by each individual parameter.

**Acknowledgments**

The authors gratefully acknowledge the funding provided by CONICYT/FONDEF D10I1086 and CONICYT-PCHA/MagisterNacional/2015 - 22150974. The authors also recognize Cementos Melon, DICTUC S.A., SIKA S.A., Mauricio Guerra and Luis Gonzalez for their contribution to this research project.

## 5. ESTIMATING THE SEGREGATION OF CONCRETE BASED ON MIXTURE DESIGN AND VIBRATORY ENERGY

Ivan Navarrete <sup>a</sup>, Mauricio Lopez <sup>a,b,c</sup>

<sup>a</sup> Department of Construction Engineering and Management, School of Engineering, Pontificia Universidad Catolica de Chile, Santiago, Chile.

<sup>b</sup> Center for Sustainable Urban development (CEDEUS), Pontificia Universidad Catolica de Chile, Vicuña Mackenna 4860, Casilla 306, Correo 22, Santiago, Chile.

<sup>c</sup> Research Center for Nanotechnology and Advanced Materials “CIEN-UC”, Pontificia Universidad Catolica de Chile, Santiago, Chile.

### **Abstract**

Controlling the segregation of concrete during construction is important for assuring design strength and durability. This paper aims to model segregation by assessing how the stability of fresh concrete is affected by the maximum size and density of aggregates, mortar viscosity, acceleration, and vibration time. The results show that aggregate properties have the greatest effect on the stability of concrete under vibration, followed by the mortar viscosity and the energy applied. Therefore, the tendency of a concrete mixture to segregate is mostly explained by the mixture design rather than by the vibration process.

### **Keywords**

Fresh concrete, vibratory energy, viscosity, rheology, aggregate size, aggregate density, image analysis.

## 5.1. Introduction

A major problem that affects fresh concrete is the tendency for coarse aggregates to separate from the mortar, causing decreased uniformity and greater variability in properties. Among the consequences of segregation, the most important are deleterious effects on the strength and durability of structures (ACI Committee 238, 2008). Because the construction workforce is generally unskilled (Finger et al., 2015), controlling the mixture design is necessary to ensure the quality of any construction.

The rheology of fresh concrete is complex because of its multi composition range and the changes in properties that occur with hydration. Previous researchers (Tattersall & Banfill, 1983) have shown that the flow behavior of fresh concrete can be reasonably approximated by the Bingham model:

$$\tau = \tau_0 + \eta_p \cdot \dot{\gamma} \quad (1)$$

Where  $\tau$  is the shear stress,  $\tau_0$  is the yield stress,  $\eta_p$  is the plastic viscosity and  $\dot{\gamma}$  is the shear rate. Thus, the flow of concrete can be described by two parameters, yield stress and plastic viscosity.

Fresh concrete can be considered as a two-phase composite material with coarse aggregate particles embedded in a mortar matrix. Beris *et al.* (Beris et al., 1985) used Bingham plastic behavior to predict how particles would settle in a fluid. A sphere will settle when the yield stress parameter ( $Y_g$ ), is less than 0.143, assuming the particle density is greater than that of the fluid; this parameter is defined as follows:

$$Y_g = \frac{3 \cdot \tau_0}{2 \cdot R \cdot |\Delta \rho| \cdot g} \quad (2)$$

Where  $|\Delta\rho|$  is the density difference between the particle and the fluid,  $R$  is the radius of the particle,  $\tau_0$  is the yield stress of the fluid and  $g$  is the gravitational acceleration. Once settling begins, the movement of a spherical particle in a Bingham fluid can be derived from the Stokes equation (Petrou, Wan, et al., 2000), defined in Eq. 3, as follows:

$$U = \frac{2 \cdot R^2 \cdot (\rho_s - \rho_f) \cdot g}{9 \cdot \eta_p \cdot C_s} \quad (3)$$

Where  $U$  is the velocity of the sphere's movement in the fluid and  $C_s$  is the Stokes drag coefficient.

Eq. 2 and Eq. 3 show that the time at which aggregate particles in fresh concrete begin moving depends on the yield stress of the mortar, the density difference between the aggregate particles and the mortar matrix, and the size of the coarse aggregates. Once movement occurs, its velocity is affected by the plastic viscosity of the mortar, the density difference between the coarse aggregate particles and the mortar and the size of the coarse aggregates. When the aggregate density is lower than that of the mortar, the principal factors that affect the stability of the fresh concrete are the same; that is, the mixture follows Eq. 3, which predicts an upward movement of coarse aggregates (Chia et al., 2005).

The vibration of concrete decreases its yield stress ( $\tau_0$ ) which makes concrete to flow easily under the same shear stress compare to the un-vibrated state (Larrard et al., 1997), at least at low shear rates (Kakuta & Kojima, 1989; Tattersall & Baker, 1988). In addition, as concrete is vibrated, the plastic viscosity at a particular shear rate is reduced. Therefore, the tendency to segregate is expected to increase when concrete is vibrated.

Previous researchers (Chia et al., 2005; B. Esmaeilkhani et al., 2014; Petrou, Harries, et al., 2000; Shen et al., 2009) have focused on the relationship between

aggregate properties and the tendency to segregate. Concrete mixtures with a greater difference in density between the coarse aggregates and mortar tend to segregate more (Chia et al., 2005; Petrou, Harries, et al., 2000). In contrast, mixtures with lower maximum size aggregates (MSA) tend to segregate less (B. Esmailkhanian et al., 2014; Shen et al., 2010).

Banfill et al. (P. F. G. Banfill et al., 1999) found that fresh concrete moves, as do the particles within it (i.e., segregation occurs) when the energy input by a vibratory wave is high enough to overcome the attraction force between the cement particles, reducing the yield stress. The energy equation postulated by Kirkham and White (Kirkham, 1963) is as follows:

$$W = c_1 \cdot m \cdot s^2 \cdot f^3 \cdot t \quad (4)$$

Where  $W$  is the energy input from vibration;  $c_1$  is a constant, depending on the stiffness and damping of the concrete;  $m$  is the concrete mass;  $s$  is the amplitude of vibration;  $f$  is the frequency of vibration; and  $t$  is the vibration time. The equation is a function of the vibratory amplitude and frequency, which are related to the maximum acceleration during the vibration ( $a_{max}$ ), calculated as follows:

$$a_{max} = 4 \cdot \pi^2 \cdot f^2 \cdot s \quad (5)$$

The effect of the vibration amplitude and frequency on the segregation of concrete have been studied separately (Grange, 2012; Mackechnie et al., 2007; Safawi et al., 2005). However, according to the authors knowledge, the relationship between the energy applied during vibration and the tendency to segregate has not been assessed.

Previous studies have examined the relationship between mixture design parameters, vibrational characteristics and the tendency of concrete to segregate. However, the interaction between mixture design parameters and vibrational characteristics requires further investigation.

## **5.2. Research Significance**

The ability of fresh concrete to remain uniform (i.e., not to segregate) during compaction is a critical issue in the design of concrete mixtures. The aim of this study is to assess the interactions between coarse aggregates, mortar viscosity and energy applied during vibration and to determine how they affect the stability of fresh concrete. This will provide a more adequate understanding and estimate of the segregation of a concrete mixture.

## **5.3. Materials and Methods**

### **5.3.1. Materials properties and mixture proportion**

All mixtures used Ordinary Portland cement (OPC), with a specific gravity of 3.14 and Blaine fineness of  $410 \text{ m}^2/\text{kg}$ , and a natural river sand with a fineness modulus of 3.18 was used as the fine aggregate (FA). The absorption of the FA was 0.97%, and the specific gravity was 2.72 at the saturated surface dry (SSD) condition.

The coarse aggregate (CA) materials included a normal-weight aggregate (NWA), specifically crushed gravel, and two lightweight aggregates (LWA), expanded shale and expanded polystyrene. The three types of CAs were sieved to obtain different single-sized aggregates. The physical properties of the single-sized NWA and LWA used in the study are given in Table 5-1. The absorption of the expanded shale was obtained after 72 hours of immersion to maximize pore saturation (ASTM, 2013).

Stereology parameters were used to measure the aggregate specific surface area (SSA) of the CA of concrete samples. The SSA was estimated from vertical uniform random (VUR) sections using an unbiased stereology technique based on cycloids.

Cycloids were used because they are considered isotropic lines on VUR sections in 3D space (Mouton, 2002a). The SSA is estimated using the following equation.

$$S_v = 2 \cdot \frac{\sum I}{\sum P \cdot l} \cdot \frac{V_c}{V_a} \quad (6)$$

Where  $\sum I$  is the number of intersections;  $\sum P$  is the number of points counted;  $l$  is the length of one test line;  $V_c$  is the volume of concrete in the sample; and  $V_a$  is the volume of aggregate in the sample.

Table 5-1: Physical properties of single-sized aggregates

Aggregate	Size (mm)	SSA (1/mm)	SSD Density (kg/m <sup>3</sup> )	Absorption, 72 hr (%)
Crushed Gravel	19.0 - 25.4	0.69	2600	2.44
	12.7 - 19.0	0.97	2630	1.74
Expanded Shale	12.7 - 19.0	0.90	1370	12.47
Expanded Polystyrene	4.8 - 9.5	1.98	15	-
	2.4 - 4.8	2.48	15	-

Three mortars were used, all of which had the same proportion of water, FA and OPC; their viscosities differed with their high range water reducer admixture (HRWA) dose. Hafidi *et al.* (Hafidi, 2013) establish that a direct relationship exists between mortar viscosity and the V-funnel flow time ( $V_{\text{time}}$ ) (ACI Committee 238, 2008). Therefore, the V-funnel test was used to characterize the viscosity of each mortar. Table 5-2 shows the  $V_{\text{time}}$  and HRWA dose by cement weight of each mortar.

Table 5-2:  $V_{\text{time}}$  and HRWA doses of each mortar

Mortar ID	HRWA (%xOPC)	V-time (s)
M1	0.250	6.8
M2	0.275	4.9
M3	0.300	3.9

Two series of concrete mixtures were prepared. Series I included five mixtures with different aggregates and mortars that were vibrated at different rates of energy and over different durations. Variations in the rate of energy applied were achieved by modifying the maximum acceleration of the vibratory table. These mixtures were used to assess the relationship between dynamic segregation and aggregate parameters (i.e., coarse aggregate size and density difference between CA and mortar), energy applied during vibration, and mortar viscosity. Series II included two additional mixtures, and these were used to validate the findings and relationships established from testing the Series I concretes.

The concrete mixtures had a water-cement ratio (W/C) of 0.45 and were composed of approximately 70% mortar and 30% CA by volume; the proportion of each constituent was kept constant in all mixtures (see Table 5-3).

Table 5-3: Concrete mixture proportions

	Mixture ID	OPC (kg/m <sup>3</sup> )	Water (kg/m <sup>3</sup> )	FA (kg/m <sup>3</sup> )	CA (kg/m <sup>3</sup> )	HRWA (kg/m <sup>3</sup> )	CA type	CA size (mm)
Series I	G-M1-1	440	200	950	789	1.1	Gravel	12.7 - 19.0
	ES-M1-1	440	200	950	411	1.1	Shale	12.7 - 19.0
	EP-M1-1	440	200	950	4.5	1.1	Exp. Pol.	4.8 - 9.5
	G-M2-1	440	200	950	441	1.21	Gravel	12.7 - 19.0
	G-M3-1	440	200	950	285	1.32	Gravel	12.7 - 19.0
Series II	EP-M1-2	440	200	950	4.5	1.1	Exp. Pol.	2.4 - 4.8
	G-M1-2	440	200	950	780	1.1	Gravel	19.0 - 25.4

Each mixture was named based on three specifications. The first letters indicate the type of aggregate used: gravel (G), expanded shale (ES) or expanded polystyrene (EP). The second letters denote the type of mortar in the mixture, M1, M2 or M3. The last number indicates whether the mixture belongs to Series I or II (1 or 2). The difference between the mixture design of the Series I and Series II mixtures is related to the aggregate sizes used.

### 5.3.2. Segregation measurement

The concrete was vibrated using a vibratory table with a frequency of 50 Hz and three different maximum accelerations ( $a_{max}$ ): 58.9 m/s<sup>2</sup> (6 g), 88.3 m/s<sup>2</sup> (9 g) and 117.7 m/s<sup>2</sup> (12 g). Table 5-4 shows the energy rates by mass achieved by each  $a_{max}$ , which were calculated by the following equation, as postulated by Kirkham and White (Kirkham, 1963):

$$W_{mr} = \frac{a_{max}^2}{16 \cdot \pi^4 \cdot f} \quad (7)$$

Where  $W_{mr}$  is the rate of energy transmitted by the mass of concrete,  $f$  is the table vibration frequency and  $a_{max}$  is the maximum acceleration of the table measured in  $m/s^2$ .

Table 5-4: Energy rate by mass with each maximum acceleration of the table

$a_{max} \left( \frac{m}{s^2} \right)$	$W_{mr} \left( \frac{J}{s \cdot kg} \right)$
58.9	0.044
88.3	0.100
117.7	0.178

Forty-five 10x20cm cylinders were cast for each mixture and these were vibrated nine different times (t) for each  $W_{mr}$ . All  $W_{mr}$  mixture samples were vibrated for 60, 90 and 120 seconds; additional times were selected to achieve three equal amounts of energy by mass ( $W_m$ ), as shown in Table 5-5. After 2 days, each concrete specimen was saw-cut through its longitudinal axis, washed to remove dust, and air-dried in the laboratory. The dry cut surfaces were imaged and used to assess the distribution of coarse aggregate.

Table 5-5: vibrations times applied to achieve the same amount of energy applied by mass with different maximum acceleration of vibratory table.

Acceleration ( $m/s^2$ )	Vibration time (s)		
	5.35 (J/kg)	10.71 (J/kg)	16.06 (J/kg)
58.9	120	240	360
88.3	53	107	160
117.7	30	60	90

The aggregate volume fraction at different heights was estimated with an unbiased stereology technique that was based on count pointing (Mouton, 2002a). Images of the tested specimens were divided into three equal sections (top, middle and bottom). For the top and bottom sections, the volume of coarse aggregate was calculated using Eq. 8, as follows:

$$V_{ai} = \frac{P_{ai}}{P_{refi}} \cdot 100\% \quad (8)$$

Where  $P_{ai}$  is the sum of the points intersecting the aggregate in section i;  $P_{refi}$  is the sum of the points intersecting section i; and  $V_{ai}$  is the aggregate volume fraction of section i.

To evaluate segregation, the volumetric index (VI), proposed by Esmailkhanian *et al* (B. Esmailkhanian et al., 2014), was calculated:

$$VI (\%) = 2 \cdot \frac{|V_{at} - V_{ab}|}{V_{at} + V_{ab}} \cdot 100\% \quad (9)$$

Where  $V_{at}$  and  $V_{ab}$  are the aggregate volume fraction of the top and bottom sections, respectively.

## 5.4. Results and Discussions

### 5.4.1. Relationship between mixture design parameters, energy applied and dynamic segregation

The aggregate parameters and VI average values for each Series I mixture,  $W_{mr}$  and vibration time are summarized in Table 5-6. The equivalent specific surface area radius ( $R_{SSA}$ ) in Table 5-6 is the ratio between the volume and the surface area of the aggregate used for each mixture; this quantity was calculated with the following equation:

$$R_{SSA} = \frac{3}{SSA} \quad (10)$$

Where SSA is the specific surface area of the aggregate. The density difference between the aggregate and mortar ( $|\Delta_\rho|$ ) in Table 5-6 was calculated as the absolute value of the difference between the SSD density of the aggregate and the density of fresh mortar.

Navarrete (Navarrete, 2015) showed that there is a linear relationship between the segregation rate and the multiplication of aggregate parameters shown in Table 5-6. Therefore, a linear relationship can also be established between the VI values and the aggregate segregation parameter ( $A_p$ ), which is defined as follows:

$$A_p = |\Delta_\rho| \cdot R_{SSA} \cdot t \quad (11)$$

However, previous studies have reported that concrete with higher  $V_{time}$  has higher viscosity and lower aggregate settling and segregation velocity (Petrou, Wan, et al., 2000; Seng, 2006). A study by Safawi *et al.* (Safawi et al., 2004) on the effect of  $V_{time}$  on the segregation tendency of vibrated concrete shows that there is a logarithmic relationship between segregation and concrete  $V_{time}$ . Thus, the viscosity segregation parameter could have a linear relationship with the VI values; this parameter is defined as follows.

$$V_p = \ln V_{time} \cdot t \quad (12)$$

Table 5-6: Aggregate parameters and volumetric index (VI) of the series I concrete mixtures

Sample ID	R <sub>SSA</sub> (mm)	Δ <sub>p</sub>   (Ton/m <sup>3</sup> )	W <sub>mr</sub> ( $\frac{J}{s \cdot kg}$ )	VI (%)								
				30 s	53 s	60 s	90 s	107 s	120 s	160 s	240 s	360 s
G-M1-1	4.35	0.42	0.044	-	-	8.2	15.3	-	17.0	-	19.8	30.9
			0.100	-	11.2	12.7	15.2	23.1	35.8	40.5	-	-
			0.178	8.4	-	27.2	34.6	-	49.5	-	-	-
ES-M1-1	3.34	0.89	0.044	-	-	39.3	69.8	-	78.7	-	106.7	169.2
			0.100	-	56.2	68.7	77.9	81.4	106	127.1	-	-
			0.178	70.4	-	133.3	154.4	-	183.1	-	-	-
EP-M1-1	1.52	2.25	0.044	-	-	46.1	55.5	-	94.9	-	151.4	189.6
			0.100	-	91.6	107.8	126.9	173.2	181.8	200.0	-	-
			0.178	78.7	-	155.8	187.8	-	200.0	-	-	-
G-M2-1	4.35	0.42	0.044	-	-	10.6	19.7	-	27.7	-	54	61.3
			0.100	-	32.3	37.8	42.1	57.2	65.6	77.3	-	-
			0.178	31.5	-	41.7	65.9	-	72.5	-	-	-
G-M3-1	4.35	0.42	0.044	-	-	10.6	18.7	-	27.7	-	54.0	105.0
			0.100	-	38.1	39.3	43.2	47.4	80.0	92.9	-	-
			0.178	35.1	-	47.6	73.8	-	98.9	-	-	-

The energy transmitted by the mass of concrete during vibration ( $W_m$ ) is an important parameter that determines its consolidation and segregation (ACI Committe 309, 2008).  $W_m$  is calculated as follows (Kirkham, 1963):

$$W_m = W_{mr} \cdot t \quad (13)$$

An analysis of variance (ANOVA) was conducted to assess the relationship between dynamic segregation and aggregate characteristics, viscosity of mortar and energy

applied. The factors used in the ANOVA were  $A_p$ ,  $V_p$  and  $W_m$ . Additionally, the products of pairs of factors and the square of each factor were used to assess interactions between factors and the nonlinear effects of factors. Thus, a total of nine factors were used in the ANOVA.

The backward elimination algorithm (Montgomery & Runger, 2003) was used to establish which of the nine factors were significant (to a level of 95%) in explaining the segregation of concrete under vibration. The results show that five factors were statistically significant:  $V_p$ ,  $A_p$ ,  $W_m$ , the square of  $V_p$  and the interaction between  $V_p$  and  $A_p$ .

The ANOVA results show that the intercept value is not different from zero. However, previous studies (Navarrete, 2015; Petrou, Harries, et al., 2000; Seng, 2006) have shown that concretes with similar mortar  $V_{timeS}$  to this study do not segregate prior to vibration. Therefore, we expect that no segregation should occur for a vibration time equal to zero, which means that the intercept value should equal zero. The significance of the square of the  $V_p$  parameter in the ANOVA shows that the assumption of a linear relationship  $V_p$  and the VI values is probably not valid. This could be due to the use of mortar  $V_{time}$  instead of concrete  $V_{time}$ , as noted by Safawi *et al.* (Safawi et al., 2004).

A multiple linear regression (MLR) model that related the VI values with the significant factors was used to assess the contribution of each significant factor to segregation. This model explained 87% of the variability of the VI values and is as follows:

$$VI_{est} = \beta_1 \cdot V_p + \beta_2 \cdot A_p + \beta_3 \cdot W_m + \beta_4 \cdot V_p^2 + \beta_5 \cdot V_p \cdot A_p \quad (14)$$

Where,  $V_p$  is in  $s \cdot Ln(s)$ ,  $V_a$  is in  $ton \cdot s \cdot mm/m^3$  and  $W_m$  is in  $(\frac{kJ}{kg})$ .

When the MLR model is used to estimate the VI values, the corresponding  $\beta_1$ ,  $\beta_2$ ,  $\beta_3$ ,  $\beta_4$  and  $\beta_5$  parameters from Eq. 14 are shown in Table 5-7. The standardized coefficients shown in Table 5-7 indicate how many standard deviations a dependent variable (i.e., a VI value) will change per standard deviation increase in the independent variable (Verdugo, Cal, & Fernández, 2005). Therefore, the standardized coefficients can be used to assess the relative effect of the independent variables on the dependent variable when the variables are measured in different units.

Table 5-7: Model summary and coefficient results of regression analysis of the VI values

	Coefficient	Standardized coefficient	Standard Error	T-Statistic	P-value	95% C.I. ( $\pm$ )
$\beta_1$	-0.630	-1.59	0.0746	-8.40	0.000	0.1490
$\beta_2$	0.640	2.23	0.0501	12.82	0.000	0.0999
$\beta_3$	5.161	0.52	0.4852	10.63	0.000	0.9685
$\beta_4$	0.001	1.13	0.0001	4.60	0.000	0.0010
$\beta_5$	-0.001	-1.44	0.0001	-6.16	0.000	0.0002

$$R^2 = 0.87$$

The fact that  $\beta_1$  is negative implies that as  $V_{\text{time}}$  increases, the dynamic segregation tendency decreases; this is expected because higher  $V_{\text{time}}$ s imply higher viscosity, more resistance to segregation, and thus less segregation. Likewise, the fact that  $\beta_5$  is negative means that the segregation tendency of aggregates that present larger size and higher density difference with the mortar are tend to be affected by the mortar viscosity.

Table 5-7 shows that aggregate characteristics have the greatest effect on the segregation tendency of concrete, followed by the mortar viscosity and the energy

applied. Therefore, the mixture design parameters are more important in controlling the segregation tendency of concrete than the vibration process.

Figure 5-1 compares the effect of vibratory energy on the VI values of three mixtures with different coarse aggregate properties and the same mortar  $V_{time}$ . Mixtures G-M1-1, ES-M1-1 and EP-M1-1 have  $|\Delta\rho| \cdot R_{SSA}$  values of 1.27 Ton·mm/m<sup>3</sup>, 2.94 Ton·mm/m<sup>3</sup> and 3.38 Ton·mm/m<sup>3</sup>, respectively. Figure 5-1 shows that adding 1 J/kg of energy increases the VI value by 2.3% for mixture G-M1-1, 9.5% for mixture ES-M1-1 and 12.7% for mixture EP-M1-1. It is apparent that mixtures with a higher  $|\Delta\rho| \cdot R_{SSA}$  value have a higher degree of segregation for a lower amount of applied vibratory energy. In contrast, the segregation tendency of mixtures with a lower  $|\Delta\rho| \cdot R_{SSA}$  value is less affected by the amount of vibratory energy applied.

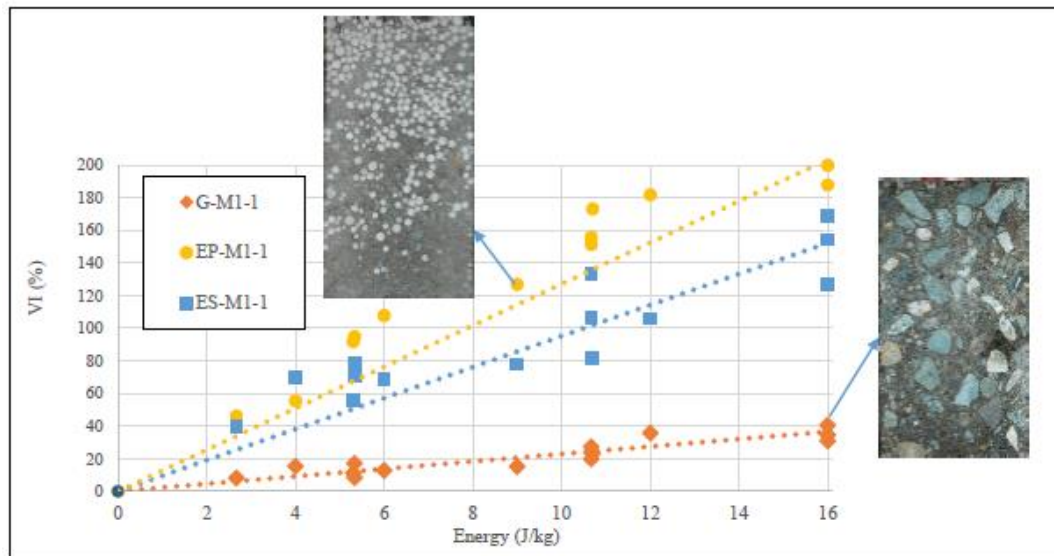


Figure 5-1: Effect of vibratory energy on segregation of mixtures with same mortar  $V_{time}$

Figure 5-2 compares the effect of vibratory energy on the VI values of three mixtures with different  $V_{time}$ s and the same coarse aggregate properties. Mixtures G-M1-1, G-

M2-1 and G-M3-1 have  $V_{timeS}$  of 6.8 s, 4.9 s and 3.9 s, respectively. Figure 5-2 shows that adding 1 J/kg of energy increases the VI value by 2.3% for mixture G-M1-1, 4.3% for mixture G-M2-1 and 5.3% for mixture G-M3-1. It can be noted that the segregation tendency of mixtures with lower  $V_{timeS}$  is more dependent on the amount of vibratory energy applied.

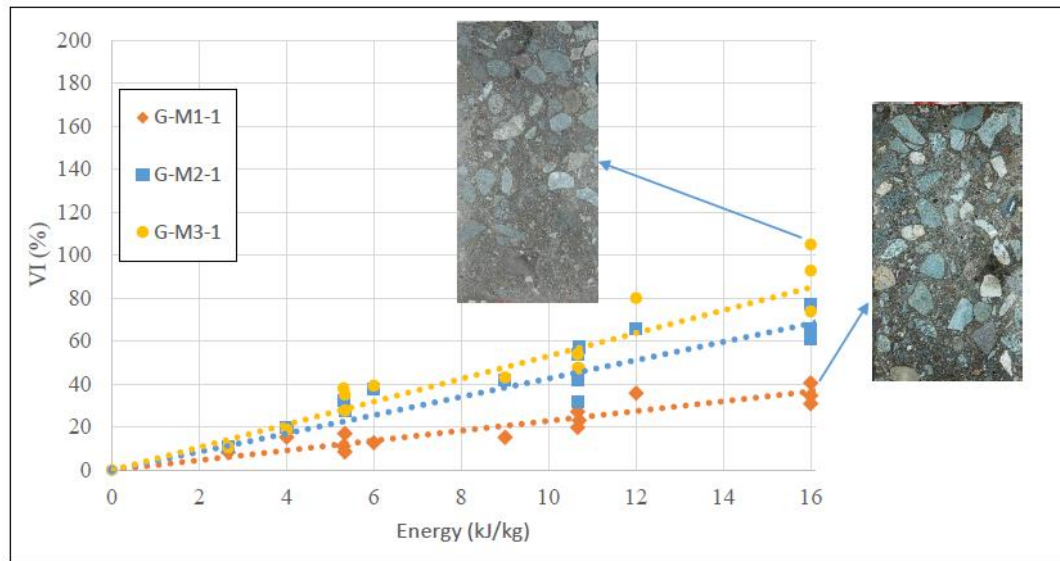


Figure 5-2: Effect of vibratory energy on segregation of mixtures with same aggregate properties.

#### 5.4.2. Segregation degree

The results of Kwasny *et al.* (Kwasny, Asce, Sonebi, & Taylor, 2012) show that a lightweight concrete can be considered to be unsegregated when the variation in aggregate content between the bottom and top sections is less than 20%. On the other hand, Esmailkhanian *et al.* (Behrouz Esmailkhanian et al., 2014) studied the dynamic segregation of self-consolidating concrete and proposed that a VI value of 25% was the limit for segregation.

This study proposes a five-level scale of segregation based on the possible VI values and the visual scale indicated by our results, and the fact that VI ranges from 0 to 200% (see Table 5-8 and Figure 5-3).

Table 5-8: VI range of segregation degrees

Segregation degree	VI range (%)
None to slight	0 - 40
Moderate	40 - 80
Severe	80 - 120
Slightly stratified	120 - 160
Highly stratified	160 - 200

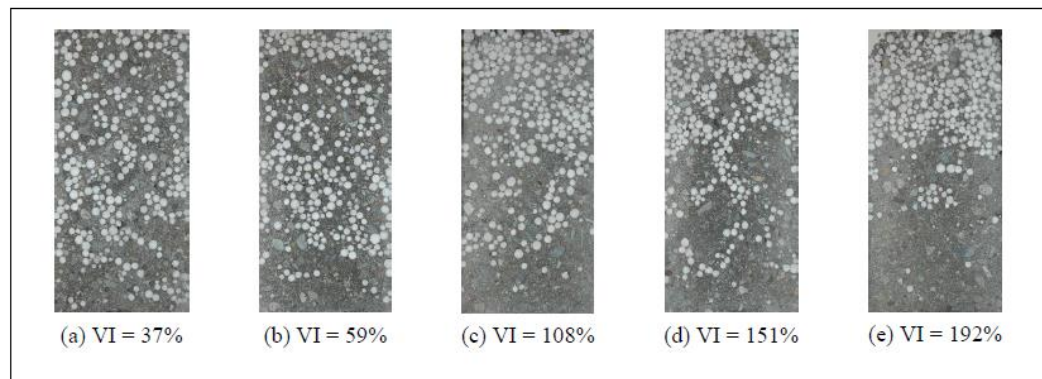


Figure 5-3: Test specimens of the EP-M1 mixture with different VI values

Figure 5-3.a shows a test specimen of the EP-M1 mixture, which has a VI value of 37%; this specimen shows slight segregation and is almost homogenous along its height. Therefore, we suggest that a VI value of 40% represents the limit for no segregation to slight segregation.

Figure 5-3.b shows a specimen with a different coarse aggregate concentration at its top and bottom, but a homogeneous distribution in the middle. Therefore, we suggest that concrete has a moderate degree of segregation between VI values of 40% and 80%. Figure 5-3.c shows a specimen with different aggregate concentrations in its bottom and top sections. In this specimen, the middle section does not show a homogeneous aggregate distribution. Thus, we suggest that severe segregation occurs between VI values of 80% and 120%.

Figure 5-3.d shows a specimen with a small amount of the CA in its bottom section and Figure 5-3.e shows a specimen with over the 90% of the CA in its top section. Mackechnie *et al.* (Mackechnie et al., 2007) defined stratified concrete as a single concrete mixture that has been vibrated to create two or more concrete layers with different mechanical (i.e., compressive strength, young modulus) and physical properties (i.e., density). Therefore, concretes with VI values between 120% and 160% can be classified as slightly stratified and concretes with VI values over 160% can be classified as highly stratified.

#### **5.4.3. Validation of MLR model for segregation**

The aggregate parameters of the two Series II concrete mixtures are summarized in Table 5-9; these mixtures were used to validate the proposed model of segregation of concrete under vibration. Both mixtures were vibrated for 30, 60, 90 and 120 seconds with a  $W_{mr}$  of  $0.178 \frac{J}{kg \cdot s}$ . The relationship between the experimental and predicted results is shown in Figure 4 and the results are summarized in Table 5-10.

Table 5-9: Aggregate parameters of concretes of series II

Mixture ID	$R_{SSA}$ (mm)	$ \Delta\rho $ (Ton/m <sup>3</sup> )
G-M1-2	4.35	0.42
EP-M1-2	1.21	2.25

Table 5-10 shows that the proposed model accurately predicts the VI values and segregation degrees of the G-M1-2 mixture for all the vibration times. For the EP-M1-2 mixture, the model tends to underestimate the VI values for vibration times greater than or equal to 60 s, but accurately predicts the degree of segregation. Consequently, the proposed model can be used to evaluate and predict with satisfactory accuracy the degree of dynamic segregation of a vibrated mixture, given the aggregate parameters, mortar viscosity, and vibratory energy applied. Additionally, considering the experimental versus predicted VI values of the Series II mixtures, the MLR model can explain 81% of the variability of the VI values of these mixtures which validates the model proposed.

Table 5-10: Experimental and predicted segregation results of Series II mixtures

Mixture ID	Time (s)	Experimental Results		Predicted Results	
		VI (%)	Segregation degree	VI (%)	Segregation degree
G- M1-2	30	33	Slight	27	slight
	60	56	Moderate	53	Moderate
	90	85	Moderate/Severe	79	Moderate/Severe
	120	100	Severe	106	Severe
EP-M1-2	30	40	Slight/Moderate	44	Slight/Moderate
	60	129	Little stratified	84	Moderate/Severe
	90	152	Little stratified	123	Severe/ Little stratified
	120	186	Highly Stratified	161	Little/ Highly Stratified

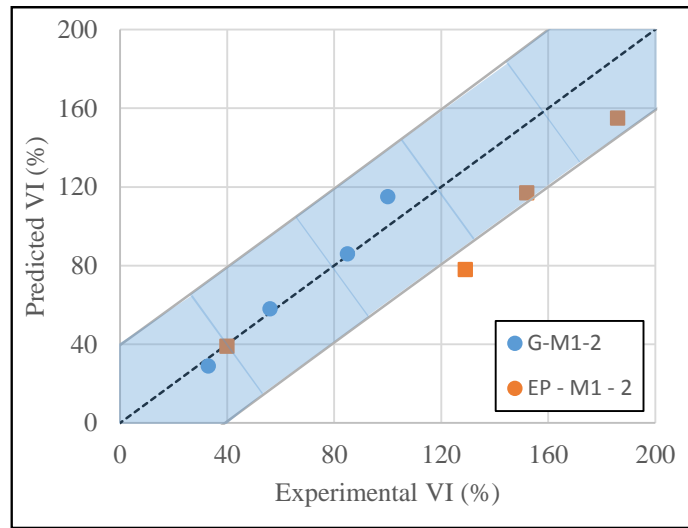


Figure 5-4: Experimental versus predicted VI values of Series II mixtures.

## 5.5. Conclusions

This study aimed to determine the main factors explaining dynamic segregation in concrete by investigating the combined effects of aggregate size, density difference between the coarse aggregates and mortar, viscosity of the mortar and energy applied during vibration by the mass of concrete. Seven mixtures were investigated with three different aggregates, viscosities, and rates of energy applied. The main conclusions of this study are:

- (1) The combined effects of the aggregate's volume-to-surface ratio and the density difference between the coarse aggregates and mortar constituted the parameter that most strongly affected the segregation tendency of concrete. This is relevant to minimizing or eliminating segregation in lightweight and heavyweight aggregate concrete mixtures and implies that the mortar viscosity and energy applied need to be considered.
- (2) The energy applied by unit mass of concrete is the parameter that least affected the segregation tendency of concrete for the mixture ranges explored in this study. This is relevant for stratified concrete design and implies that the mixture design is more important than the vibration process.
- (3) Analysis of variance showed that there is a correlation between the effect of aggregate parameters and mortar viscosity in the segregation of concrete during vibration. This is relevant when using lightweight and heavyweight aggregates with large MSAs in normal weight mortar and implies that the viscosity of mortar must be considered to minimize or eliminate segregation in those cases.
- (4) The significance of the squared  $V_{\text{time}}$  parameter in the ANOVA shows that the assumption of a logarithmic relationship between  $V_{\text{time}}$  and VI values is not valid.

(5) This study proposes five segregation degrees to evaluate the segregation of concrete. The mixtures analyzed in this study exemplified the different levels of segregation. This means that unsegregated concrete or stratified concrete can be obtained by controlling the mixture design of concrete or the amount of energy applied during vibration.

### **Acknowledgments**

The authors gratefully acknowledge the funding provided by CONICYT/FONDEF D10I1086 and CONICYT-PCHA/MagisterNacional/2015 - 22150974. The authors also recognize Cementos Melon, DICTUC S.A., SIKA S.A., Mauricio Guerra and Luis Gonzalez for their contribution to this research project.

## 6. STRATIFIED CONCRETE: CONSTRUCTION, FLEXURAL BEHAVIOR, ANALYSIS AND DESIGN APPROACH

Ivan Navarrete <sup>a</sup>, Yahya Kurama <sup>b</sup>, Matias A. Hube <sup>c</sup>, and Mauricio Lopez <sup>a,d,e</sup>

<sup>a</sup> Department of Construction Engineering and Management, School of Engineering, Pontificia Universidad Catolica de Chile, Santiago, Chile

<sup>b</sup> Department of Civil & Environmental Engineering & Earth Sciences, School of Engineering, University of Notre Dame, South Bend, IN, United State

<sup>c</sup> Department of Structural and Geotechnical Engineering, School of Engineering, Pontificia Universidad Catolica de Chile, Santiago, Chile.

<sup>d</sup> Center for Sustainable Urban development (CEDEUS), Pontificia Universidad Catolica de Chile, Vicuña Mackenna 4860, Casilla 306, Correo 22, Santiago, Chile

<sup>e</sup> Research Center for Nanotechnology and Advanced Materials “CIEN-UC”, Pontificia Universidad Catolica de Chile, Santiago, Chile

### **Abstract**

Stratified concrete poses as a promising alternative for layered construction. Its fresh and hardened properties have been studied at the material level; however, structural behavior in steel reinforced specimens have not been studied yet. This paper focuses on the flexural behavior of four reinforced stratified concrete (RSC) specimens. Structural specimens with two stratified concrete mixture designs were tested and compared against the predictions from a fiber element model and the rectangular stress-block method from ACI 318-14. The test results suggest that RSC presents similar damage mode and different failure mode than ordinary reinforced concrete (ORC). The fiber

element model accurately predicted the flexural behavior of RSC while the rectangular stress-block underestimated the flexural strength of RSC by 26%, which is similar to that obtained for ORC. Therefore, stratified concrete specimens can be designed using both fiber element and rectangular stress-block approaches.

### **Keywords**

OpenSees, fiber element model, segregation, lightweight concrete, rectangular stress-block, ductility.

## **6.1. Introduction**

Environmental impact and energy consumption have become increasing concerns around the world. If we follow the current path, greenhouse gas and energy-related CO<sub>2</sub> emissions will rise by 52% and 78%, respectively, from 2005 to 2050 (OECD, 2009). As a major contributor to these emissions, buildings consume between 20% and 40% of the primary energy worldwide (Pérez-Lombard et al., 2008) and the thermal performance of the building envelope is the main factor affecting its energy (Cárdenas, Muñoz, Riquelme, & Hidalgo, 2015).

Concrete, the most widely used construction material worldwide, excels in mechanical properties and constructability, but lacks in thermal performance. Stratified concrete, developed by Mackechnie *et al* (Mackechnie et al., 2007), is produced from a single concrete mixture that is over vibrated to produce a normal-weight concrete layer and a light-weight concrete layer. Normal-weight concrete provides the benefit of thermal mass but has little insulating ability (Kim et al., 2003). On the other hand, light-weight concrete offers limited thermal mass but has excellent insulating properties due to its high air content (Sengul et al., 2011).

Building envelopes composed of both layers optimize thermal performance and reduce energy consumption (Saevarsdottir, 2008).

Few studies have characterized the mechanical properties of stratified concrete. Grange (Grange, 2012) investigated the viability of producing stratified concrete panels in an industrial setting. The research focused on the vibration process and optimization of concrete stratification. Saevarsdottir (Saevarsdottir, 2008) studied the mechanical, serviceability and durability performance of stratified concrete panels. However, the mechanical properties of the test specimens were limited to concrete without reinforcement.

Unskilled workforce and lack of supervision are the principal causes of quality problems in building construction (Finger et al., 2015). On the other hand, the use of precast panel systems offers the opportunity to control the quality of the end product to a very high degree, because the panels are cast by specialized precast concrete plants in a controlled environment (Dayton Superior Corporation, 2015). This is especially important for stratified concrete applications, due to the need to control the vibration process to achieve the desired stratification. However, when the panel is lifted from its horizontal casting position, its dead weight induces flexural stresses that may exceed in-situ construction strengths. Building on the previous material level studies on the mechanical properties of stratified concrete (Grange, 2012; Mackechnie et al., 2009, 2007; Mackechnie & Saevarsdottir, 2007), new research is needed to understand the flexural behavior of reinforced stratified concrete structures.

Test results from Grange (Grange, 2012) showed no delamination between stratified concrete layers. Lightweight concrete layers presented compressive strength lower than 10 MPa and normal-weight concrete layers presented compressive strength higher than 30 MPa in all specimens tested by Saevarsdottir (Saevarsdottir, 2008) and Grange (Grange, 2012). On the other hand, ACI318-14 (ACI Committee 318, 2014) requires a minimum compressive concrete strength of 17 MPa to ensure good

bonding between steel and concrete. Therefore, stratified concrete is especially attractive for insulated reinforced concrete slabs where the normal-weight concrete layer ensures a strong medium to place the reinforcement and the lightweight concrete layer provides the insulation.

Considering that stratified concrete is a novel material, it is necessary to understand if common design methods (i.e. rectangular stress-block method of ACI318 (ACI Committee 318, 2014)) and analytical models for ORC can be used to design RSC. Mullapudi (Mullapudi, 2010) and Taucer *et al.* (Taucer, Spacone, & Filippou, 1991) have demonstrated that the fiber element model is one of the most promising techniques because it is less computationally demanding than finite element models while also more sophisticated than other available models for the nonlinear analysis of reinforced concrete structures. The fiber element model requires details of the section, geometry of the structural member, and properties of the materials. An important limitation of most fiber element models is that reinforcement bond slip and nonlinear shear deformations cannot be modeled (Jiang & Kurama, 2010); however, its effectiveness for axial-flexure-controlled reinforced concrete members has been demonstrated for ORC (Morgen & Kurama, 2008). Further investigation is needed to validate it for RSC analysis as well.

## **6.2. Research Significance**

The objective of this study is to assess the flexural behavior, design, and analysis of RSC structures. Monotonic load tests were conducted on four RSC specimens. Two specimens were cast for each of two different stratified concrete mixture designs and tested under 4 point bending. The test results were evaluated based on the load and deflection at yielding and ultimate points. A fiber element model was developed to analyze the load-deflection behavior of the specimens. Moreover, the rectangular stress-block method was used to estimate the ultimate load of the specimens and validated based on the measured results.

### 6.3. Research program

#### 6.3.1. Experimental program

Two specimens were cast for each of two different stratified concrete mixture designs (SCG and SCS). The main difference between the mixtures is that SCG was made with normal-weight coarse aggregate (crushed gravel) while SCS was made with lightweight coarse aggregate (expanded shale). The physical properties of the aggregates are shown in Table 6-1. The absorption of expanded shale was obtained after 72-hour immersion to maximize the pore saturation (ASTM, 2013).

Table 6-1: Coarse aggregate properties

	Crushed gravel	Expanded Shale
Maximum nominal size (mm)	25.4	19.0
SSD density (ton/m <sup>3</sup> )	2.68	1.40
Water absorption (%)	1.62	12.32
Gradation (sieve opening)	Cumulative passing (%)	Cumulative passing (%)
3/4 in. (19 mm)	83.9	98.1
1/2 in. (12.5 mm)	31.6	46.7
3/8 in. (9.5 mm)	12.8	12
No. 4 (4.75 mm)	0.6	0.2

Ordinary Portland cement (OPC) with specific gravity of 3.14 and Blaine fineness of 410 m<sup>2</sup>/kg and natural river sand with fineness modulus of 3.18 as fine aggregate (FA) were used for all mixtures. The absorption of FA was 0.97%, and specific gravity was 2.72 at the saturated surface dry (SSD) condition. Also, high range water reducer admixture (HRWA) was used in a dose of 0.25% by cement weight. Mixture proportions for SCG and SCS are presented in Table 6-2.

Table 6-2: Concrete mixture proportions

Materials	Quantity (kg/m <sup>3</sup> )	
	SCG	SCS
Cement	400	400
Microsilica	30	30
Water	200	200
Sand	625	625
Crushed gravel	350	-
Expanded shale	-	206
Expanded polystyrene	4.3	4.3
HRWA	1.0	1.0

The reinforcement was A440-280 steel with a nominal strength of 280 MPa. The actual yield and ultimate strength obtained from tensile testing of the bars were 370 MPa and 580 MPa, respectively, and the actual yield strain was 0.0017. The stress-strain relationships measured from these tests are shown in Figure 6-1.

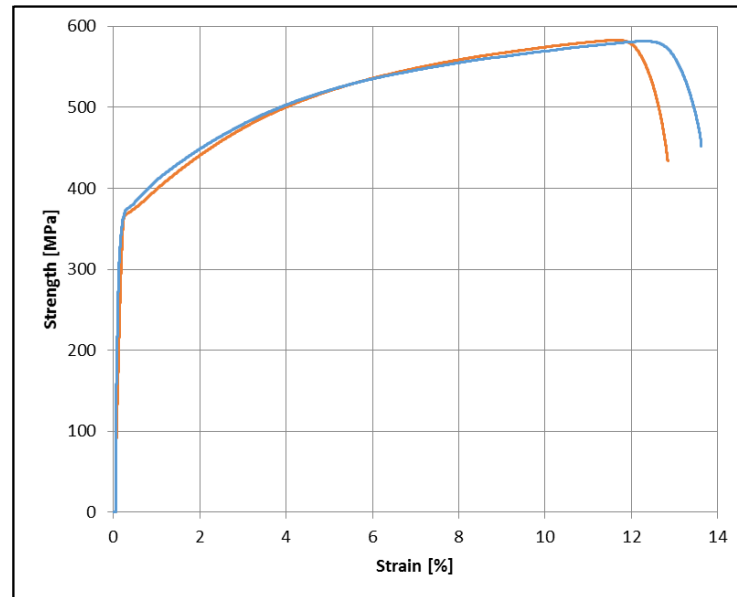


Figure 6-1: Measured stress-strain relationships for steel reinforcement

Schematic front and cross-sectional views of the test specimens are shown in Figure 6-2. Two 8 mm diameter bars were used as tensile reinforcement. The cross-sectional dimensions and reinforcement were selected to represent typical wall panel and slab construction, with no transverse reinforcement since shear failure was not critical.

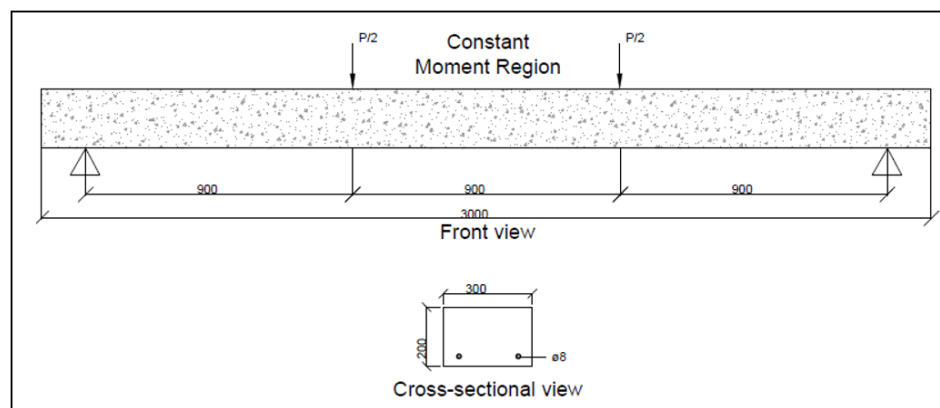


Figure 6-2: Elevation and cross-sectional views of the test specimens (units in mm).

### 6.3.1.1. Reinforced stratified concrete specimens building process

The mixing of SCG and SCS batches was carried out in a 200 liter pan mixer according to the protocol shown in Table 6-3. Immediately following mixing, a 200x300x3300 mm formwork was filled and vibrated using an internal concrete vibrator for 30 seconds at each of the points depicted in Figure 6-3. After the end of the vibration process, a steel slide was inserted vertically into the fresh concrete to obtain a 200x300x3000 mm element for flexure testing and a 200x300x300 mm prism for the measurement of the stratified layer properties.

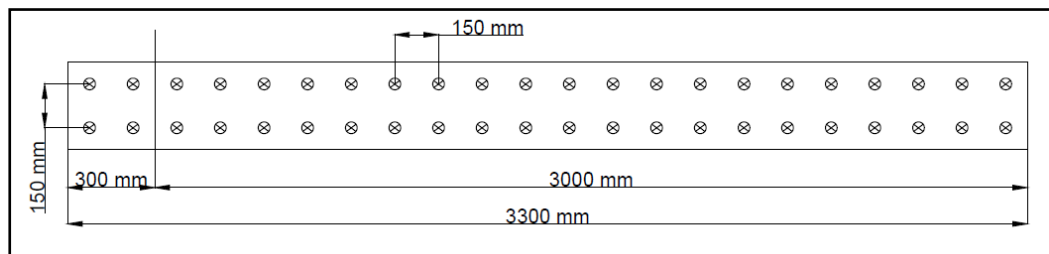


Figure 6-3: Plan view of specimens showing vibration points for stratification

Table 6-3: Mixing protocol for stratified concrete mixtures.

Time (min:sec)	Action
0:00	Mix aggregates and expanded polystyrene with 1/3 water
2:00	Mix rest of dry ingredients with 2/3 superplasticizer and rest of water
5:00	Stop to scrape sides of mixer
7:00	Mix rest of superplasticizer
10:00	Stop mixing

### **6.3.1.2. Measurement of stratified concrete layers properties**

The different layers resulting from the vibration of each specimen were determined by determining the segregation profile over the member height (Safawi et al., 2005). This profile was drawn by plotting the value of  $(G/C)_i / (G/C)_{ave}$  against the height of the element, where  $(G/C)_i$  is the percentage of expanded polystyrene at height  $i$  and  $(G/C)_{ave}$  is the average of  $(G/C)_i$  factors. The percentage of expanded polystyrene at the different heights was estimated using an unbiased stereology technique based on count pointing (Mouton, 2002b). The results from these measurements are discussed in Section 4 later.

Once the different layers of concrete were identified, the compressive strength and elastic modulus of each layer were measured at an age of 100 days (which is the same as the testing age of the flexural specimens) on samples obtained from the 200x300x300 mm prism. The compressive strength was measured on nine 50x50x50 mm cubes and the Young's modulus was measured on three 50x100 mm core samples for each layer. The Young's modulus was determined based on ASTM C469 (Test et al., 2006) by applying up to 33% of the maximum compressive strength and measuring the average strain using three gauges and a data acquisition system.

### **6.3.1.3. Flexural test set-up and instrumentation**

Monotonic loading was applied using two 50 kN capacity hydraulic jacks at two points, producing a constant moment region of 900 mm in the middle of the 2700 mm clear span, as shown Figure 6-1 and Figure 6-4. The total load applied by the hydraulic jacks was measured continuously with a load cell. The mid-span deflection and longitudinal strains were measured using displacement transducers. The displacement transducers for longitudinal strain were placed at different heights over the mid-span of each specimen. However, the flexural cracks did not develop within

the gauge length of these transducers, and thus, the longitudinal strains across the cracked regions of the beams could not be measured.

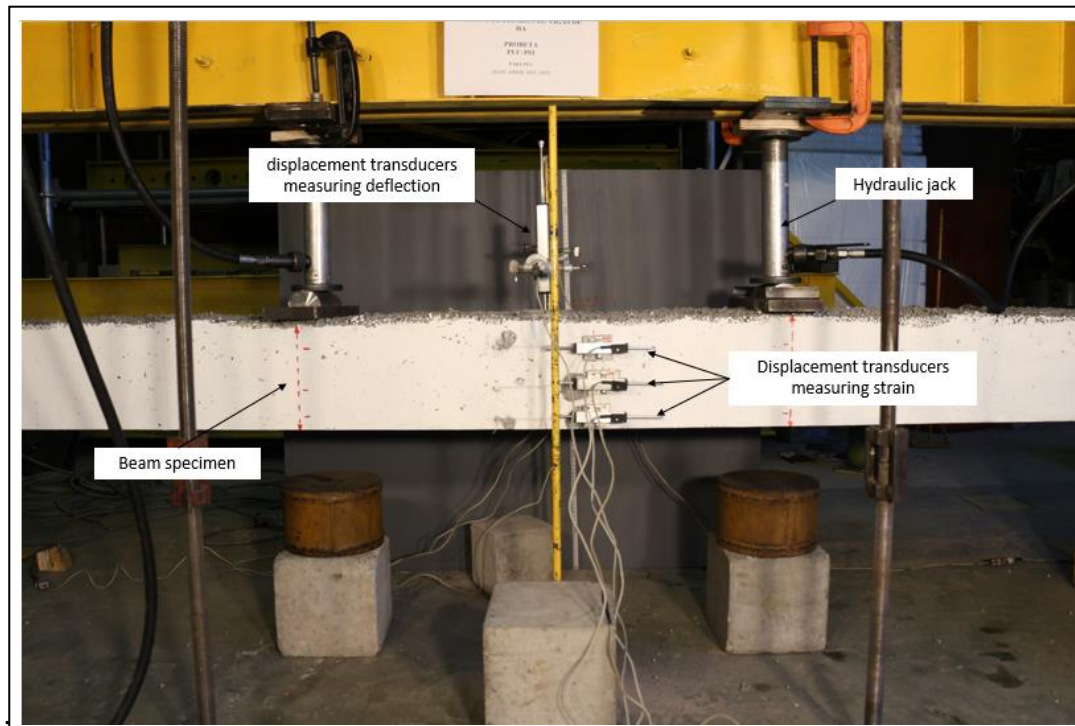


Figure 6-4: Test-setup used for flexural loading.

### 6.3.2. Analytical modelling

Fiber element models of the RSC specimens were developed using the non-linear force-based beam-column element in the open source object-oriented nonlinear structural analysis software, OpenSees (Mckenna, Fenves, Scott, & Jeremic, 2000). Shear deformations were not included in the analysis.

Each concrete layer and steel reinforcement in the RSC cross sections of each specimen was modeled using fibers to capture the stress variation across the depth. Each cross section was discretized into a total of fifty fibers. The stress-strain

behavior of the concrete was defined using the Concrete04 Popovics material model (Popovics, 1973) in OpenSees, while the stress-strain behavior of the steel reinforcement was defined using the Reinforcing Steel material model with isotropic strain hardening. The properties of each concrete layer in each specimen and of the steel reinforcement were obtained from laboratory tests as explained previously.

The length of each specimen was divided into six elements of 450 mm length, as shown in Figure 6-5. For each of these elements, six integration points using Legendre integration quadrature were defined along the length. Modeling assumptions for plane sections remaining plane and perfect bond between steel reinforcement and concrete were maintained throughout the analysis.

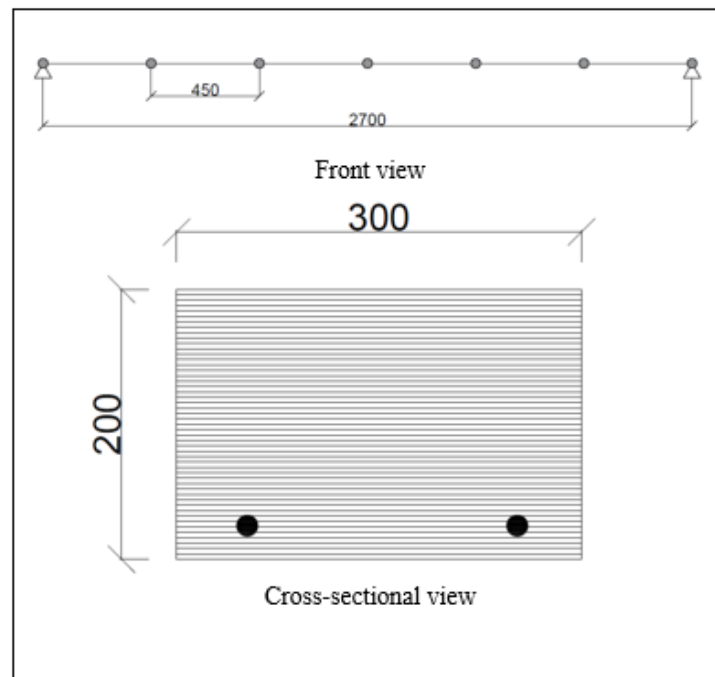


Figure 6-5: Fiber element model of reinforced stratified concrete specimens

## 6.4. Results and Discussions

### 6.4.1. Stratified concrete layers properties

Figure 6-6.a and Figure 6-6.b show the cross-sections used in the stereology analyses of the SCG and SCS specimens, respectively, and Figure 6-7.a and Figure 6-7.b show the resulting average expanded polystyrene segregation profiles, respectively. SCG specimens showed two regions with different polystyrene contents over the height and the SCS specimens showed three regions with different polystyrene contents. Accordingly, the SCG specimens were classified as two-layer concrete specimens and the SCS specimens were classified as three-layer concrete specimens. The measured compression strengths of these distinct concrete layers are discussed later.

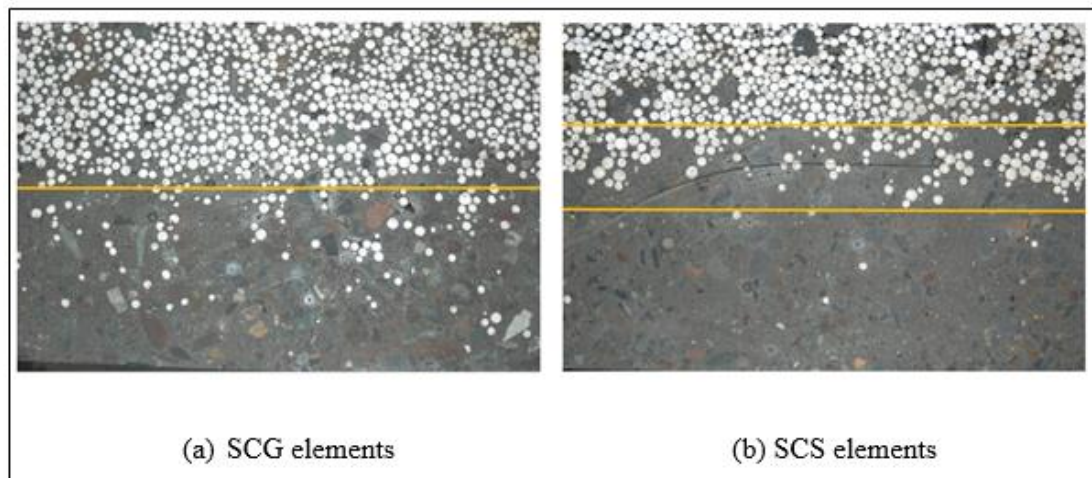


Figure 6-6: Stratified concrete cross-sections

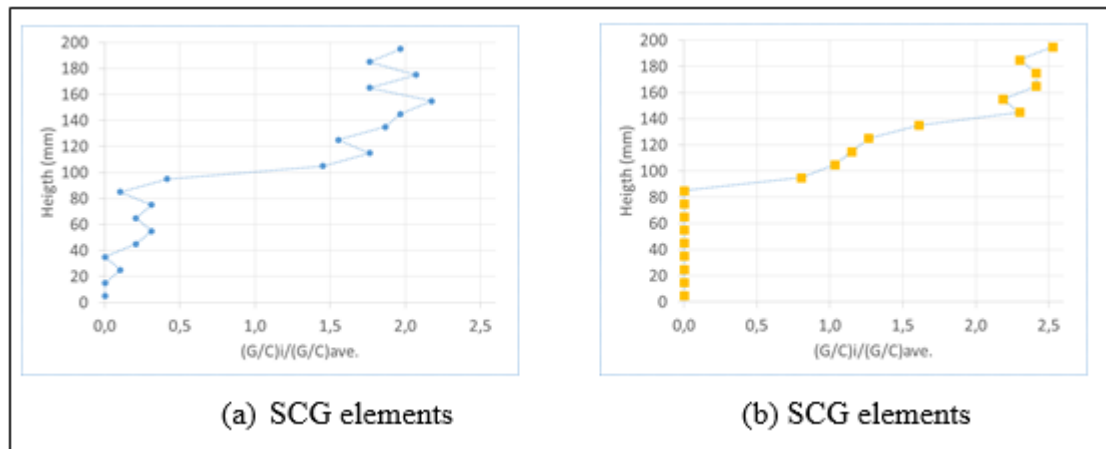


Figure 6-7: Average segregation profile

Compressive strength, Young's modulus, and density of each concrete layer were measured as listed in Table 6-4. The top and mid concrete layers of the SCS specimens and the top layer of the SCG specimens were classified as low-strength light-weight concrete (Chandra & Berntsson, 2003). On the other hand, the bottom concrete layer of each specimen was classified as normal-weight structural concrete (Mehta & Monteiro, 2014).

Table 6-4: Summary of stratified concrete layers properties

Sample ID	SCG-1		SCG-2		SCS-1			SCS-2		
	Top	Bottom	Top	Bottom	Top	Mid	Bottom	Top	Mid	Bottom
Width (mm)	100	100	100	100	50	60	90	50	60	90
Density (Ton/m <sup>3</sup> )	1.15	2.12	1.29	2.29	0.69	1.42	2.12	0.87	1.34	1.97
f <sub>c</sub> (MPa)	8.9	39.9	8.1	54.3	3.6	14.6	53	3.2	14	58.6
E (GPa)	6.7	38.5	5.4	49.9	3.4	10.6	19	4.7	13.8	33.2

The stratification process was controlled by the rheological properties of the mortar, the density and gradation of the coarse aggregates, and the amount of vibratory

energy applied (Mackechnie et al., 2007; Navarrete, 2015). A paired t-test (Kennedy & Neville, 1966) was used to compare the compressive strengths of nine cube samples from the top and bottom concrete layers of each SCG specimen and from the top, mid, and bottom concrete layers of each SCS specimen. The results showed a significant difference between the compressive strengths of the identified concrete layers with a significance level of 0.05. These comparisons verified the classification of the SCG specimens as two-layer concrete and the SCS specimens as three-layer concrete.

#### **6.4.2. Experimental study**

Typical failure mode and crack pattern observed within the constant moment region of the test specimens are shown in Figure 6-8. All four specimens developed progressive vertical flexural cracks (mainly in the constant moment region) with increasing deflection, but maintained their structural integrity and post-peak behavior with appreciable deflection. The damage, characterized by increasing crack widths, was concentrated in a localized region of the specimens prior to failure. This damage progression was similar to the behavior observed for ORC specimens by Mertol et al (Mertol, Baran, & Bello, 2015). However, the ultimate failure of all four SRC specimens occurred due to fracture of the reinforcing bars, which was different from the failure due to concrete crushing of the ORC specimens with similar reinforcement ratio observed by Mertol et al (Mertol et al., 2015).



Figure 6-8: Typical crack pattern and failure mode of flexural tests.

The measured load-deflection curves from the flexural tests are shown in Figure 6-9, with the results summarized in Table 6-5. The yield strength ( $P_y$ ) and yield deflection ( $\delta_y$ ) were defined when the bottom displacement transducer (see Figure 6-4) located at the level of longitudinal steel reached the measured steel yield strain of 0.17%. The ultimate strength ( $P_u$ ) was defined as the maximum total load resisted by the specimens ( $P$  in Figure 6-2) and the ultimate deflection ( $\delta_u$ ) was defined as the deflection at failure due to steel fracture. The secant stiffness in Table 6-5 was calculated as the slope of the straight line between the origin and the point representing 50% of the ultimate load of the load-deflection curve. The displacement ductility was calculated as the ratio between the ultimate deflection and the yield deflection.

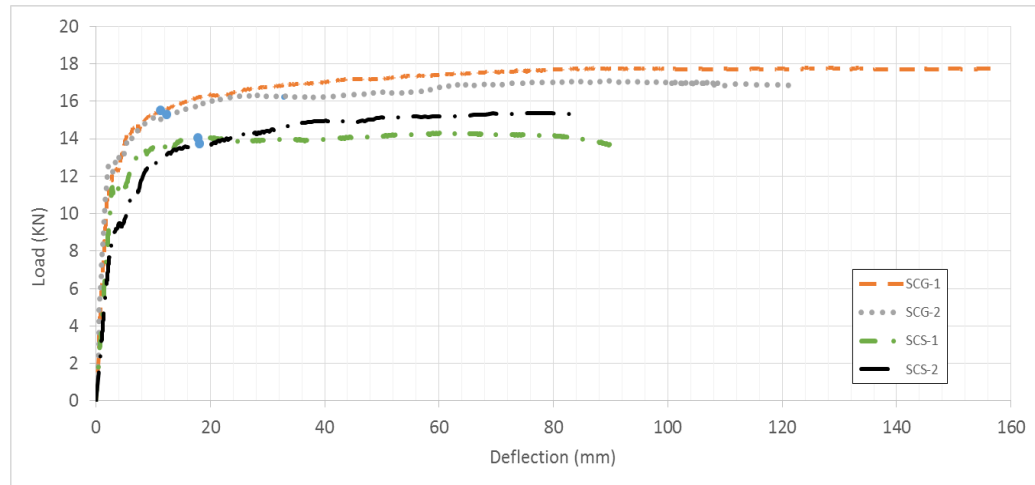


Figure 6-9: Measured load-deflection curves

Table 6-5: Summary of flexural test results

Sample ID	$P_y$ (kN)	$P_u$ (kN)	$\delta_y$ (mm)	$\delta_u$ (mm)	Secant Stiffness (kN/mm)	Displacement ductility
SCG-1	15.52	17.78	11.3	152.1	5.52	13.46
SCG-2	15.30	17.08	12.3	122.2	7.12	9.93
Average SCG	15.41	17.43	11.8	137.2	6.32	-
SCS-1	14.04	14.30	17.8	91.3	4.13	5.13
SCS-2	13.74	15.34	18.1	87.3	3.26	4.83
Average SCS	13.89	14.82	17.9	89.3	3.70	-

For specimens SCG-1 and SCG-2, yielding of the steel ( $P_y$ ) occurred at 15.52 kN and 15.30 kN, respectively, with an average of 15.41 kN, whereas for specimens SCS-1 and SCS-2, yielding of the steel occurred at 14.04 and 13.74 kN, respectively, with an average of 13.89 kN. The average ultimate loads ( $P_u$ ) were 17.43 kN and 14.82 kN for the SCG and SCS specimens, respectively. Therefore, the SCG specimens developed, on average, 10% higher yield load and 15% higher ultimate

load with respect to the SCS specimens. The yield deflection ( $\delta_y$ ) for specimens SCG-1 and SCG-2 were 34% lower than that of specimens SCS-1 and SCS-2, while the average ultimate deflection for the SCG specimens was 35% greater than that of the SCS specimens. These comparisons show that the SCG specimens demonstrated better structural performance than the SCS specimens. This is mainly attributed to the compressive strength of the top layer concrete in the SCG specimens, which was about 1.5 times the compressive strength of the top layer concrete in the SCS specimens.

The displacement ductility was determined as 13.46 and 9.83 for specimens SCG-1 and SCG-2, respectively, and as 5.13 and 4.83 for specimens SCS-1 and SCS-2, respectively. Tests conducted by Mertol et al (Mertol et al., 2015) have shown that the ductility of a reinforced concrete member is related to the reinforcement ratio. The reinforcement ratio of all four SCS and SCG specimens were 0.002. The ductility of ORC specimens with comparable reinforcement ratios tested by Mertol et al (Mertol et al., 2015) was around 11. Therefore, the SCG specimens achieved higher ductility while the SCS specimens achieved lower ductility than ORC specimens with similar reinforcement ratios.

Regarding thermal performance, the density of the top layer concrete in the SCS specimens was about 36% lower than that of the top layer concrete in the SCG specimens. Ozkan *et al.* (Sengul et al., 2011) studied the effect of expanded polystyrene on the thermal conductivity of light-weight concrete, where a reduction of 36% in concrete density (due to higher content of expanded polystyrene) was found to reduce thermal conductivity by 50%. Therefore, considering the thicknesses of the concrete layers, it is expected that the SCS specimens present a lower thermal conductivity than the SCG specimens.

### **6.4.3. Analytical Study**

This section compares the results from the fiber element analyses with the measured behaviors of the test specimens. The analytical and measured load-deflection curves are depicted in Figure 6-10, with the analytical yield and ultimate loads and deflections summarized in Table 6-6 and compared with the corresponding measured values from Table 6-5. The error in the predicted yield load as compared to the test data was smaller than 15%. Previous researchers (Astorga, Santa, & Lopez, 2013; Mertol et al., 2015; Yoo, Ryu, & Choo, 2015) have reported errors in the fiber element model prediction for the yield load of ORC below 40% in all cases and below 20% in 80% of the cases. Therefore, the errors in the fiber element model prediction for the yield loads of the SRC test specimens in this research are in the same order of magnitude as errors previously reported for ORC specimens.

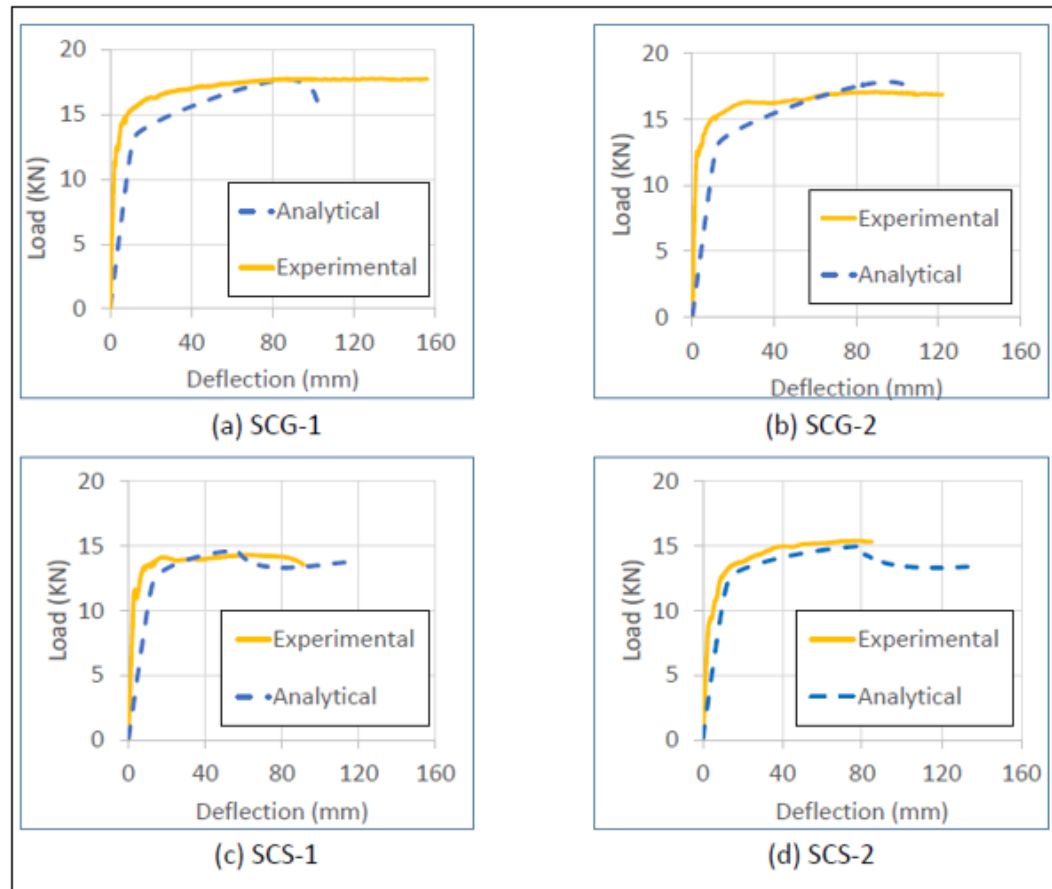


Figure 6-10: Comparison Analytical prediction and Experimental load-deflection curves

Table 6-6: Summary of Analytical prediction of load test results and corresponding errors

Sample ID	$P_y$ (N)	Error in $P_y$ (%)	$P_u$ (N)	Error in $P_u$ (%)	$\delta_y$ (mm)	Error in $\delta_y$ (%)	$\delta_u$ (mm)	Error in $\delta_u$ (%)
SCG1	13.3	-14.0	17.7	-0.56	12.5	10.6	101.8	-33.1
SCG2	13.2	-13.6	17.8	4.33	13.0	5.7	106.6	-12.8
SCS1	12.6	-10.4	14.6	2.24	14.4	-19.1	122.1	33.7
SCS2	12.7	-7.9	15	-2.35	14.3	-20.9	142.3	63.0

The fiber element model overestimated the yield deflection of the SCG specimens and underestimated the yield deflection of the SCS specimens by less than 11% and 21%, respectively. Previous studies (Astorga et al., 2013; Mertol et al., 2015; Yoo et al., 2015) have shown errors in the fiber element model prediction for the yield deflection of ORC between 10% and 60%, with 90% of the cases below 30%. Therefore, the errors in the predicted yield deflections for the RSC specimens in this research are similar to the errors for previous ORC specimens.

The errors in the predicted ultimate loads as compared to the test results were smaller than 4.5%. By considering that the difference between the ultimate loads within each pair of SCG specimens and each pair of SCS specimens were 4.1% and 7.9%, respectively, the analytical prediction errors were lower than the variability presented in specimens built from the same batch.

The errors in the predicted ultimate deflections remained lower than 34%, except for specimen SCS-2 for which the error was high. The errors presented by previous researchers on the ultimate deflection of ORC specimens (Astorga et al., 2013; Mertol et al., 2015; Yoo et al., 2015) have been between 13% and 38%. Therefore, the errors in the predicted ultimate deflections from the fiber element modeling of the RSC specimens were generally in the same order of magnitude of the errors for previous ORC specimens. These results show that the fiber element modeling technique was able to capture the behavior of the stratified reinforced concrete test specimens with a similar accuracy as has been generally obtained in previous studies of ordinary reinforced concrete specimens.

## **6.5. Stratified concrete rectangular stress-block**

The measured flexural strength of the RSC specimens was compared to the flexural strength calculated by the rectangular stress-block method from ACI318-14 (ACI Committee 318, 2014) using the actual material properties for concrete and steel.

This method was used even though the concrete strengths of the top and mid layers in the test specimens were less than the minimum concrete strength of 17 MPa required by ACI318-14. It should be noted that the method should only be used when shear failure is not dominant (Wang & Salmon, 1998), as was the case of the test specimens herein.

Figure 6-11 shows the tested RSC cross sections together with the analytical conditions for strain and stress considering a rectangular stress-block at the ultimate load stage.

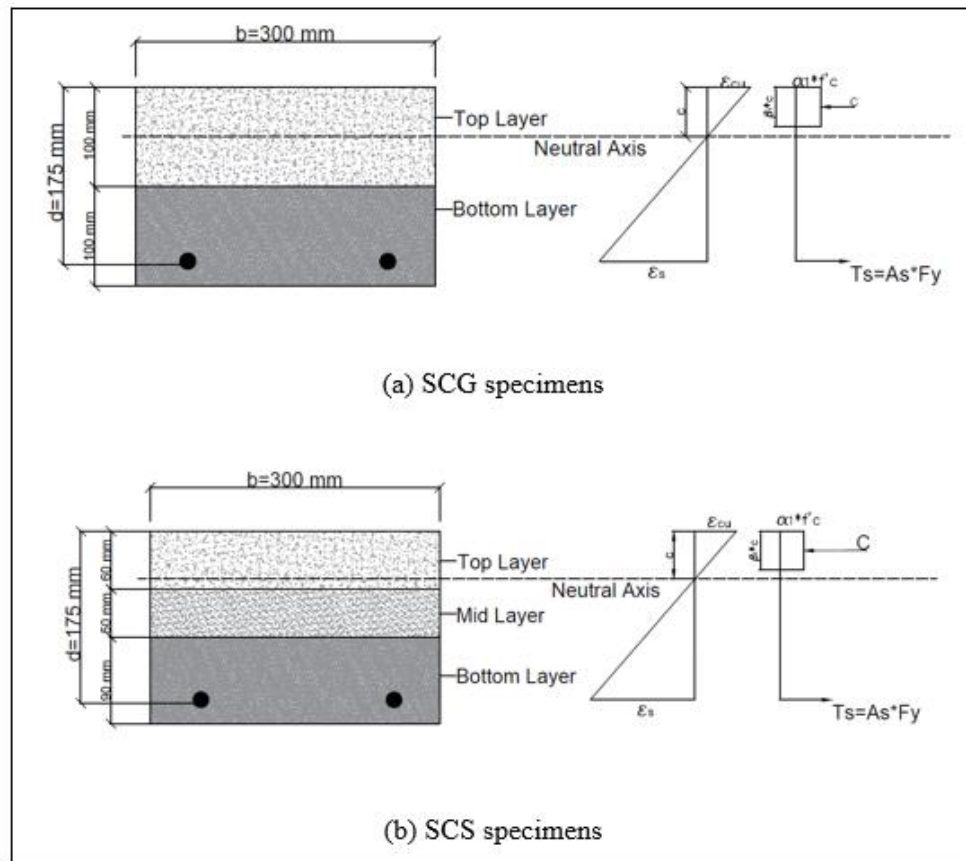


Figure 6-11: Stress and strain distribution for RSC specimens

As suggested by ACI318 (American Concrete Institute, 2008), the nominal flexural strength ( $M_n$ ) of an ordinary singly-reinforced concrete cross-section can be calculated as:

$$M_n = A_s \cdot f_y \cdot \left( d - \frac{\beta_1 \cdot c}{2} \right) \quad (1)$$

$$c = \frac{A_s \cdot f_y}{\beta_1 \cdot \alpha_1 \cdot f'_c \cdot b} \quad (2)$$

where  $b$  is the section width;  $c$  is the distance from the neutral axis to the extreme compression fiber of the concrete;  $\beta_1$  is taken as 0.85 for  $f'_c \leq 28$  MPa and reduced by 0.05 for every 7 MPa over 28 MPa; and  $\alpha_1$  is taken as 0.85 for normal-weight concrete.

For computation of  $M_n$ , ACI318-14 (ACI Committee 318, 2014) assumes that the tensile strength of the concrete can be neglected. By considering the relatively low tensile reinforcement ratio of the tested specimens, only the top concrete layer was in compression at the ultimate load stage. Therefore, Eq. 1 was used with  $f'_c$  corresponding to the compressive strength of the top layer. Since the top layer of the test specimens was lightweight concrete,  $\alpha_1$  and  $\beta_1$  were taken as 0.80 and 0.85 (Nahhas, 2013), respectively.

Comparisons between the experimentally determined  $\mu$  (corresponding to the measured ultimate load,  $P_u$ ; see Eq. 3) and the strength calculated using the rectangular stress-block method are summarized in Table 6-7. The ultimate load calculated for the SCG specimens was 12.95 kN, while the measured ultimate loads for SCG-1 and SCG-2 were 17.43 kN and 14.82 kN, respectively. Likewise, the ultimate load calculated for the SCS specimens was 11.00 kN, while the measured ultimate loads for SCS-1 and SCS-2 were 14.30 kN and 15.34 kN, respectively. Therefore, the rectangular stress-block method underestimated the measured strengths of the RSC specimens by approximately 26%.

$$M_u(\text{kN} \cdot \text{m}) = \frac{P_u}{2} \cdot 9 \quad (3)$$

Table 6-7: Comparison between rectangular stress-block method and experimental test results.

Mixture	$P_u^{exp}$ (kN)	$M_u^{exp}$ (kN*m)	$M_n^{ACI 318}$ (kN*m)	Neutral Axis depth (mm)	Error in predicted ultimate moment (%)
SCG	17.4	7.8	5.8	21.5	-25.7
SCS	14.8	6.7	5.0	49.3	-25.8

The rectangular stress-block model underestimated the ultimate load of the test specimens mainly because of the assumed elastic-plastic behavior of the reinforcing steel. As the failure of all four specimens was controlled by steel fracture, strain hardening of the steel is relevant for the flexural strength, which was not included in the predictions.

The estimated neutral axis depth (Table 6-7) from the rectangular stress block was smaller than the height of the top layer (Table 6-4) in all of the specimens tested. Therefore, only the top layer of each specimen was in compression at the ultimate load stage, which confirms the assumption used in the calculation of  $M_n$ . If this condition is not fulfilled, different stress block parameters should be used.

According to the results of (Astorga et al., 2013; Peng, Ho, & Pam, 2011; Yoo et al., 2015; Zareh, 1971), the rectangular stress-block method of ACI318-14 (ACI Committee 318, 2014) underestimated the ultimate flexural strength of ordinary reinforced concrete specimens by 10% to 30%, with 75% of the cases below 20%. Therefore, the errors in the predicted ultimate load of the RSC specimens in this research fall within the same order of magnitude of errors in using the rectangular stress-block method to estimate the ultimate load of ORC.

## 6.6. Conclusions

This research investigated the flexural behavior of reinforced stratified concrete (RSC) specimens made from two types of concrete mixtures where a light-weight concrete layer was created at the top and a normal-weight concrete layer was created at the bottom. Four reinforced specimens with 200x300x3000 mm dimensions were tested. The load-deflection behaviors of the specimens were measured and compared with the predictions from a fiber element model as well as from the rectangular stress-block method in ACI 318-14. Important conclusions from the research are listed below. It should be noted that these conclusions may be limited to the specimens and materials tested. More research is needed on stratified reinforced concrete structures.

(1) The reinforced stratified concrete (RSC) specimens demonstrated progression of damage through flexural cracking similar to ordinary reinforced concrete (ORC). The relatively low reinforcement ratio of the specimens resulted in ultimate failure due to the fracture of the reinforcing bars, without significant concrete crushing.

(2) The fiber element models were able to predict the measured behavior of the RSC test specimens with similar accuracy as has been obtained for ORC in previous research. It is concluded that this modeling technique can be used to predict the flexural behavior of reinforced stratified concrete wall panels and slabs.

(3) The rectangular stress-block design method can be used to conservatively estimate the flexural strength of RSC.

(4) The stratified reinforced concrete specimens showed no unexpected behavior under flexural loading, which supports the potential use of this novel material in building structures without the need for special design and analysis procedures.

## **Acknowledgments**

The authors gratefully acknowledge the funding provided by CONICYT/FONDEF D10I1086, CONICYT-PCHA/MagisterNacional/2015 - 22150974, and the University of Notre Dame-Pontificia Universidad Catolica de Chile dual program. The authors also recognize Cementos Melon, DICTUC S.A., SIKA S.A., Mauricio Guerra and Luis Gonzalez for their contributions to this research project.

## 7. CONCLUSIONS AND RECOMENDATIONS

### 7.1. Conclusions

- The segregation rate produced during vibration was shown to be independent of the time of vibration, so it is an intrinsic fresh property of the concrete mixture and can be used to characterize its behavior under vibration.
- The volume-to-surface area ratio of coarse aggregate explained the segregation rate of concrete more precisely than MSA, meaning that the shape of the aggregate plays a significant role in segregation. That is, segregation can be reduced by either reducing MSA or increasing the angularity of coarse aggregate.
- As the density difference between coarse aggregate and mortar increases, the volume-to-surface area ratio becomes more significant in explaining the segregation rate. This is relevant for stratified concrete mixture design and implies that maximum size and shape of the coarse aggregate need to be specially considered to assess an adequate stratification.
- The segregation tendency of a concrete mixture is more related to the combined effect of its volume-to-surface ratio and density difference between coarse aggregate and mortar than by each individual parameter. This result accept hypothesis 1.
- It was develop an analytical model that relates segregation tendency to mixture design parameters (mortar viscosity, density difference between mortar and coarse aggregate and specific surface area of coarse aggregate) and vibration characteristics (energy applied by mass of concrete). This model explained the 87% of the variability of the segregation. These results accept hypothesis 2.

- The combined effect of aggregate volume-to-surface ratio and density difference between coarse aggregate and mortar is the parameter that most affects the segregation tendency of concrete. On the other hand, the energy applied by mass of concrete is the parameter that less affects the segregation tendency of concrete. This is relevant for stratified concrete and implies that the mixture design is more important than the vibration process to achieve a good stratification.
- The reinforced stratified concrete (RSC) specimens demonstrated progression of damage through flexural cracking similar to ordinary reinforced concrete (ORC). The relatively low reinforcement ratio of the specimens resulted in ultimate failure due to the fracture of the reinforcing bars, without significant concrete crushing.
- The comparison of fiber element model with the test data of reinforced stratified concrete specimens shows that the analytic results accurately predict the behavior of RSC specimens. This model can be used to prevent problems during the building process of reinforced stratified concrete panels walls. These results accept hypothesis 3.
- The rectangular stress-block design method underestimates the flexural strength of RSC by near 26% and ORC by less than 30%. Therefore, the rectangular stress-block method present similar results in both cases and can be used for preliminary design of RSC specimens. These results accept hypothesis 3.
- Stratified concrete presents a normal behavior under flexure loads; therefore this novel material does not need special design and analysis procedures and could be used safely in reinforced concrete structures.

## 7.2. Recommendations

- All the samples used to assess the effect of mixture design parameters and vibration characteristics in segregation tendency of concrete had the same height. Future research could evaluate the relationship between samples height and segregation tendency.
- The results of the present research show that the relationship between mortar  $V_{\text{time}}$  and segregation tendency is not logarithmical, as was proposed by previous researchers. It is recommended to characterize the relationship between mortar  $V_{\text{time}}$  and segregation tendency in future studies.
- The viscosity of mortar was measured using the V-funnel test. However, this method provide an indirect measurement of the viscosity. It is recommended to characterize the relationship between direct measured viscosity and segregation tendency in future researchers.
- The energy applied during vibration was measured with an external accelerometer. Nevertheless, the energy perceived by the concrete is different due to energy losses. Future research could characterize the effect of concrete perceived energy in segregation using embedded accelerometers.
- This study propose an analytical model that assess the effect of coarse aggregate properties, mortar viscosity and vibration characteristics in vibration tendency. However, the obtained results are limited by the use of one type of coarse aggregate. Future research could evaluate the effect of use two types of coarse aggregate in segregation tendency.

- Flexural behavior of reinforced stratified concrete was achieved from monotonic load test. However, due to the cost of the test no control specimen of ordinary reinforced concrete (ORC) was tested. Future research could compare the behavior of RSC beams with ORC of similar dimensions and reinforcement.
- Reinforced stratified concrete (RSC) present higher ductility than ordinary reinforced concrete. This was attributed to the higher crushing strain of lightweight concretes. However, this property was not measure in the present study. Future research could measure lightweight concrete crushing strain and asses its effect in stratified concrete ductility.
- In the present research only the flexural behavior of RSC was characterized and modeling. Further research is require to understand the structural behavior of RSC. Future studies could analyze the shear behavior or the neutral axis of RSC.

## REFERENCES

- ACI Committe 309. (2008). *Report on behavior of Fresh Concrete During Vibration*. Farmington Hills.
- ACI Committee 238. (2008). *Report on Measurements of Workability and Rheology of Fresh Concrete*. Farmington Hills.
- ACI Committee 318. (2014). *ACI 318-14: Building code requirements for structural concrete and commentary*. Farmington Hills.
- American Concrete Institute. (2008). *318-08 Building Code Requirements for Structural Concrete*. ACI.
- ASTM. (2013). *C1761 Standard Specification for Lightweight Aggregate for Internal Curing of Concrete* (Vol. i).
- Astorga, A., Santa, H., & Lopez, M. (2013). Behavior of a concrete bridge cantilevered slab reinforced using NSM CFRP strips. *Construction and Building Materials*, 40, 461–472. <http://doi.org/10.1016/j.conbuildmat.2012.09.095>
- Banfill, P. F. G. (2006). Rheology of fresh cement and concrete. *Rheology Review*, 2006, 61–130. <http://doi.org/10.4324/9780203473290>
- Banfill, P. F. G., Xu, Y., & Domone, P. L. J. (1999). Relationship between the rheology of unvibrated fresh concrete and its flow under vibration in a vertical pipe apparatus. *Magazine of Concrete Research*, 51(3), 181–190. <http://doi.org/10.1680/mac.1999.51.3.181>
- Bellamy, L. A., & McSaveney, L. G. (2003). *FRST - Future Building Systems Research Proposal*. Christchurch.
- Beris, A. N., Tsamopoulos, J. A., Armstrong, R. C., & Brown, R. A. (1985). Creeping motion of a sphere through a Bingham plastic. *Journal of Fluid Mechanics*, 158, 219–244.
- Cárdenas, J. P., Muñoz, E., Riquelme, C., & Hidalgo, F. (2015). Simplified life cycle assessment applied to structural insulated panels homes Análisis de ciclo de vida simplificado aplicado a viviendas de paneles SIP ( structural insulated panels ). *Revista Ingeniería de Construcción*, 30, 33–38.
- Cement Concrete & Aggregates Australia. (2002). *Thermal Benefits of Solid*

*Construction.*

Chandra, S., & Berntsson, L. (2003). *Lightweight Aggregate Concrete - Science, technology and Applications*. (V. S. Ramachandran, Ed.). New York: William Andrew Publishing.

Chia, K., Kho, C., & Zhang, M. (2005). Stability of fresh lightweight aggregate concrete under vibration. *ACI Materials Journal*, 102(5), 347–354. Retrieved from <http://www.concrete.org/Publications/InternationalConcreteAbstractsPortal.aspx?m=details&i=14714>

Corporación de Desarrollo Tecnológico. (2010). *Estudio de usos finales y curva de la conservación de la energía en el sector residencial*. Santiago.

Dayton Superior Corporation. (2015). *Tilt-up Handbook*.

Esmailkhanian, B., Feys, D., Khayat, K. H., & Yahia, A. (2014). New Test Method to Evaluate Dynamic Stability of Self-Consolidating Concrete. *ACI Materials Journal*, 111(3). <http://doi.org/10.14359/51686573>

Esmailkhanian, B., Khayat, K. H., Yahia, a., & Feys, D. (2014). Effects of mix design parameters and rheological properties on dynamic stability of self-consolidating concrete. *Cement and Concrete Composites*, 54, 21–28. <http://doi.org/10.1016/j.cemconcomp.2014.03.001>

EURIMA. (2007). U-values in Europe. Retrieved November 1, 2015, from <http://www.eurima.org/u-values-in-europe>

Fang, Z., Li, N., Li, B., Luo, G., & Huang, Y. (2014). The effect of building envelope insulation on cooling energy consumption in summer. *Energy and Buildings*, 77, 197–205. <http://doi.org/10.1016/j.enbuild.2014.03.030>

Ferraris, C. F. (1999). Measurement of the rheological properties of high performance concrete: State of the art report. *Journal of Research of the National Institute of Standards and Technology*, 104(5), 461. <http://doi.org/10.6028/jres.104.028>

Finger, F. B., González, M. S., & Kern, A. P. (2015). Control of Finished Work – Final Quality Inspection in a Social Housing Project Control de la obra terminada – inspección final de calidad en un proyecto de interés social, 30, 147–153.

Grange, B. P. (2012). *Investigating the Commercial Viability of Stratified Concrete Panels*. University of Canterbury.

Gundersen, H. J. G., Jensen, E. B. V, Kiêu, K., & Nielsen, J. (1999). The efficiency of

- systematic sampling in stereology - Reconsidered. *Journal of Microscopy*, 193(3), 199–211. <http://doi.org/10.1046/j.1365-2818.1999.00457.x>
- Hafidi, a A. (2013). Correlation Between Viscosity and V - Funnel Flow. *International Journal of Advanced Technology & Engineering Research*, 3(1), 103–108.
- Jiang, H., & Kurama, Y. (2010). Analytical Modeling of Medium-Rise Reinforced Concrete Shear Walls. *ACI Structural Journal*, 107(4), 400–410.
- Kakuta, S., & Kojima, T. (1989). Effect of Chemical Admixtures on the Rheology of Fresh Concrete During Vibration. *ACI Materials Journal*, 119, 189–208.
- Kennedy, J. B., & Neville, A. (1966). *Basic statistical methods for engineers and scientists*.
- Kibert, C. J. (2012). *Sustainable Construction: Green Buiding Design and Delivery*.
- Kim, K.-H., Jeon, S.-E., Kim, J.-K., & Yang, S. (2003). An experimental study on thermal conductivity of concrete. *Cement and Concrete Research*, 33(3), 363–371. [http://doi.org/10.1016/S0008-8846\(02\)00965-1](http://doi.org/10.1016/S0008-8846(02)00965-1)
- Kirkham, R. H. H. (1963). *The Compaction of Concrete by Surface Vibration*. Budapest.
- Kwasny, J., Asce, S. M., Sonebi, M., & Taylor, S. E. (2012). Influence of the Type of Coarse Lightweight Aggregate on Properties of Semilightweight Self-Consolidating Concrete, (December), 1474–1483. [http://doi.org/10.1061/\(ASCE\)MT.1943-5533.0000527](http://doi.org/10.1061/(ASCE)MT.1943-5533.0000527).
- Kwasny, J., Asce, S. M., Sonebi, M., Taylor, S. E., Bai, Y., Owens, K., & Doherty, W. (2012). Influence of the Type of Coarse Lightweight Aggregate on Properties of Semilightweight Self-Consolidating Concrete, (December), 1474–1483. [http://doi.org/10.1061/\(ASCE\)MT.1943-5533.0000527](http://doi.org/10.1061/(ASCE)MT.1943-5533.0000527).
- L’Hermite, R., & Touron, G. (1948). *The rheology of fresh concrete and vibration*.
- Larrard, F. de, Hu, C., Sedran, T., Sztikar, J. C., Joly, M., Claux, F., & Derkx, F. (1997). A New Rheometer for Soft-to-Fluid Fresh Concrete. *ACI Materials Journal*, 94(3), 234–243. <http://doi.org/10.14359/304>
- Leith, D. (1987). Drag on Nonspherical Objects. *Aerosol Science and Technology*, 6(2), 153–161. <http://doi.org/10.1080/02786828708959128>
- Lesovik, R. V., Botsman, L. N., Tarasenko, V. N., & Botsman, N. (2014). ENHANCEMENT OF SOUND INSULATION OF FLOORS USING LIGHTWEIGHT

CONCRETE BASED ON NANOSTRUCTURED GRANULAR AGGREGATE, 9(10), 1789–1793.

Mackechnie, J. R., Bellamy, L. A., & McSaveney, L. G. (2009). Development of stratified concrete wall panels. In *Proceeding of the 11th International Conference on Non-conventional Materials and technologies*. Bath, UK.

Mackechnie, J. R., & Saevarsdottir, T. (2007). *NEW INSULATING PRECAST CONCRETE PANELS*. Christchurch.

Mackechnie, J. R., Saevarsdottir, T., & Bellamy, L. A. (2007). Stratified Precast Concrete Panels for Buildings. *Concrete Plant International*.

Mckenna, F., Fenves, G. L., Scott, M. H., & Jeremic, B. (2000). *Open System for Earthquake Engineering Simulation (OpenSees)*. Berkeley, CA.

Mehta, P. K., & Monteiro, P. J. M. (2014). *Concrete - microstructure, properties, and materials* (fourth). Mc Graw Hill Education.

Mertol, H. C., Baran, E., & Bello, H. J. (2015). Flexural behavior of lightly and heavily reinforced steel fiber concrete beams. *Construction and Building Materials*, 98, 185–193. <http://doi.org/10.1016/j.conbuildmat.2015.08.032>

MINVU. (2011). *Ordenanza General de Urbanismo y Construcciones*. Santiago.

Montgomery, D. C., & Runger, G. C. (2003). *Applied Statistics and Probability for Engineers* (3rd ed.). Phoenix.

Morgen, B. G., & Kurama, Y. C. (2008). Seismic Response Evaluation of Posttensioned Precast Concrete Frames with Friction Dampers. *Journal of Structural Engineering*, 134(1), 132–145. [http://doi.org/10.1061/\(ASCE\)0733-9445\(2008\)134:1\(132\)](http://doi.org/10.1061/(ASCE)0733-9445(2008)134:1(132))

Mouton, P. R. (2002a). *Principles and Practices of Unbiased Stereology*. Baltimore.

Mouton, P. R. (2002b). Volume. In *Principles and Practices of Unbiased Stereology*. (pp. 88–112).

Mullapudi, T. (2010). *Seismic analysis of reinforced concrete structures subjected to combined axial, flexure, shear and torsional loads*.

Nahhas, T. M. (2013). Flexural Behavior and Ductility of Reinforced Lightweight Concrete Beams with Polypropylene Fiber, *1*(February), 4–10.

National Precast Concrete Association. (2006). *The little book of concrete - A guide to the one hundred advantages of precast concrete*. Indianapolis.

Navarrete, I. (2015). *STRATIFIED CONCRETE: UNDERSTANDING ITS STRATIFICATION PROCESS AND MODELLING ITS STRUCTURAL BEHAVIOR*. Pontificia Universidad Catolica de Chile.

OECD. (2009). *Climate Change: Meeting the Challenge to 2050*.

Peng, J., Ho, J. C. M., & Pam, H. J. (2011). Modification on Equivalent Stress Block of Normal-Strength Concrete by Incorporating Strain Gradient Effects, *14*, 2246–2253. <http://doi.org/10.1016/j.proeng.2011.07.283>

Pérez-Lombard, L., Ortiz, J., & Pout, C. (2008). A review on buildings energy consumption information. *Energy and Buildings*, *40*(3), 394–398. <http://doi.org/10.1016/j.enbuild.2007.03.007>

Petrou, M. F., Harries, K. A., Gadala-Maria, F., & Kolli, V. G. (2000). A unique experimental method for monitoring aggregate settlement in concrete. *Cement and Concrete Research*, *30*(5), 809–816. [http://doi.org/10.1016/S0008-8846\(00\)00223-4](http://doi.org/10.1016/S0008-8846(00)00223-4)

Petrou, M. F., Wan, B., Gadala-Maria, F., Kolli, V. G., & Harries, K. a. (2000). Influence of mortar rheology on aggregate settlement. *ACI Structural Journal*, *97*(4), 479–485.

Phillips, R. J., Armstrong, R. C., Brown, R. a, Graham, A. L., & Abbott, J. R. (1992). A constitutive equation for concentrated suspensions that accounts for shear-induced particle migration. *Physics Of Fluids A Fluid Dynamics*, *4*(1), 30. <http://doi.org/10.1063/1.858498>

Popovics, S. (1973). A numerical approach to the complete stress-strain curve of concrete. *Cement and Concrete Research*. [http://doi.org/10.1016/0008-8846\(73\)90096-3](http://doi.org/10.1016/0008-8846(73)90096-3)

Saevarsdottir, T. (2008). *The structural , serviceability and durability performance of variable density concrete panels Table of Contents*.

Safawi, M. I., Iwaki, I., & Miura, T. (2004). The segregation tendency in the vibration of high fluidity concrete. *Cement and Concrete Research*, *34*(2), 219–226. [http://doi.org/10.1016/S0008-8846\(03\)00249-7](http://doi.org/10.1016/S0008-8846(03)00249-7)

Safawi, M. I., Iwaki, I., & Miura, T. (2005). A study on the applicability of vibration in fresh high fluidity concrete. *Cement and Concrete Research*, *35*(9), 1834–1845. <http://doi.org/10.1016/j.cemconres.2004.10.031>

Seng, C. K. O. K. (2006). *Workability and Stability of Lightweight Aggregate Concrete From Rheology Perspective for the Degree of Doctor of Philosophy*.

- Sengul, O., Azizi, S., Karaosmanoglu, F., & Tasdemir, M. A. (2011). Effect of expanded perlite on the mechanical properties and thermal conductivity of lightweight concrete. *Energy and Buildings*, 43(2-3), 671–676. <http://doi.org/10.1016/j.enbuild.2010.11.008>
- Shen, L., Struble, L., & Lange, D. (2009). Modeling dynamic segregation of self-consolidating concrete. *ACI Materials Journal*, 106(4), 375–380. <http://doi.org/10.1016/j.conbuildmat.2014.11.010>
- Shen, L., Struble, L., & Lange, D. (2010). Modeling Dynamic Segregation of Self-Consolidating Concrete, (106), 375–380.
- Singh, S. B., Munjal, P., & Thammishetti, N. (2015). Role of water/cement ratio on strength development of cement mortar. *Journal of Building Engineering*, 4, 94–100. <http://doi.org/10.1016/j.jobe.2015.09.003>
- Sousa, H., Carvalho, A. P. O., & Melo, A. F. (2004). A New Sound Insulation Lightweight Concrete Masonry Block. Design and Experimental Characterization. *13th International Brick and Block Masonry Conference Amsterdam*, 1–8.
- Tattersall, G. H., & Baker, P. H. (1988). The effect of vibration on the rheological properties of fresh concrete. *Magazine of Concrete Research*, 40(143), 79–89.
- Tattersall, G. H., & Banfill, P. F. G. (1983). *The Rheology of Fresh Concrete*.
- Taucer, F. F., Spacone, E., & Filippou, F. C. (1991). *a Fiber Beam-Column Element for Seismic Response Analysis*. *Engineering*. Retrieved from [www.ce.berkeley.edu/~filippou/Research/.../Reports/EERC91-17.pdf](http://www.ce.berkeley.edu/~filippou/Research/.../Reports/EERC91-17.pdf)
- Test, C. C., Drilled, T., Elements, C., Drilled, U., Cores, C., & Concrete, C. (2006). Standard Test Method for Static Modulus of Elasticity and Poisson ' s Ratio of Concrete, *i*, 2–6. <http://doi.org/10.1520/C0469-02E01.2>
- The Concrete Centre. (2007). *High performance buildings using concrete frames and cladding*.
- Verdugo, M. V., Cal, M. I., & Fernández, C. M. (2005). *Análisis econométrico: una aproximación práctica con Shazam*. DELTA.
- Wang, C.-K., & Salmon, C. G. (1998). Strength of Rectangular Sections in Bending. In *Reinforced Concrete Design* (pp. 46–104).
- Yang, L., & Li, Y. (2008). Cooling load reduction by using thermal mass and night ventilation. *Energy and Buildings*, 40(11), 2052–2058.

<http://doi.org/10.1016/j.enbuild.2008.05.014>

Yoo, S.-W., Ryu, G.-S., & Choo, J. F. (2015). Evaluation of the effects of high-volume fly ash on the flexural behavior of reinforced concrete beams. *Construction and Building Materials*, 93, 1132–1144. <http://doi.org/10.1016/j.conbuildmat.2015.05.021>

Zareh, M. (1971). Comparative study of lightweight and normal weight concrete in flexure.

**APPENDICES**

## 8. APPENDICES

### 8.1. Images of laboratory equipment



Figure 8-1: Vibratory table and accelerometer



Figure 8-2: Mortar V-funnel Test

## 8.2. Volumetric Index measurement procedure

This section describe the procedure used to measure the volumetric index, which was used to characterize the segregation tendency of the concrete.

At the age of 2 days, the concrete specimens were saw-cut through the longitudinal axis, washed from dust, and air dried in the laboratory. The dry cut surfaces were photographed and used to measure the distribution of coarse aggregate.

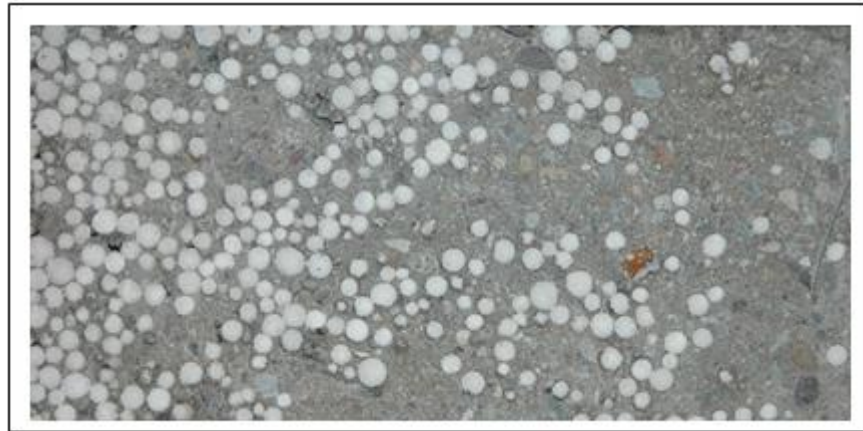


Figure 8-3: Example of saw-cut of cylinder sample

- Using Image-J program, a point's grid is putting over the picture.

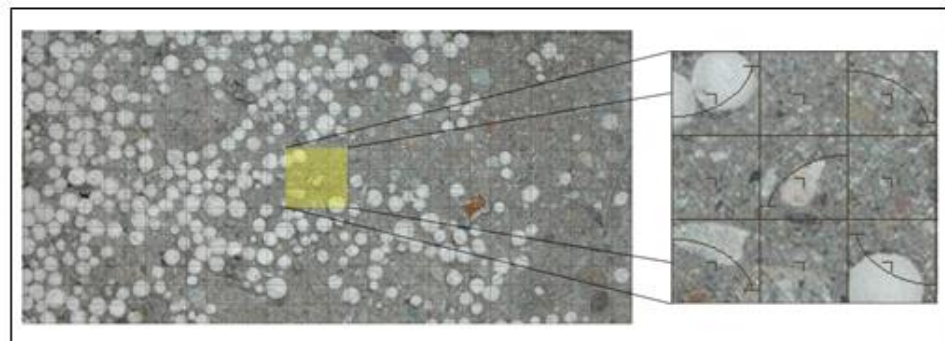


Figure 8-4: Example of saw-cut of cylinder sample with point's grid.

- Tested specimens' photographs were divided into three equals sections (top, mid and bottom). For top and bottom sections the volume of coarse aggregate was calculated by using the following equation:

$$V_{ai} = \frac{P_{ai}}{P_{refi}} \cdot 100\% \quad (1)$$

Where  $P_{ai}$  is the sum of the points reaching the aggregate in section i;  $P_{refi}$  is the sum of the points reaching the section i and  $V_{ai}$  is the aggregate volume fraction of section i.

- Then, the volumetric index was calculated by using the following equation:

$$VI (\%) = 2 \cdot \frac{|V_{at} - V_{ab}|}{V_{at} + V_{ab}} \cdot 100\% \quad (2)$$

Where  $V_{at}$  and  $V_{ab}$  are the aggregate volume fraction of the top and bottom section, respectively.

### 8.3. Fiber-element model of flexural behavior of reinforced stratified concrete

This section shows the code of the fiber-element model used to analyze the flexural behavior of reinforced stratified concrete.

```
# SET UP -----
# units: kgf, cm, sec

wipe;                # clear memory of all past model
definitions

model BasicBuilder -ndm 2 -ndf 3;    # Define the model builder

GEOMETRY -----

set HCol 20;          # Column Depth
set BCol 30;          # Column Width

# nodal coordinates:
node 1 0 0;           # node number, X, Y
node 2 0 45;
node 3 0 90;
node 4 0 135;
node 5 0 180;
node 6 0 225;
node 7 0 270;

# Single point constraints -- Boundary Conditions
fix 1 1 0 0;          # node DX DY RZ
fix 7 1 1 0;          # node DX DY RZ

# Define ELEMENTS & SECTIONS -----
----
set ColSecTag1 1;     # assign a tag number to the column section

# define section geometry
set barAreaCol 1.0053;    # 2 phi 8 A44
```

```

# MATERIAL parameters -----

set IDconcU1 1;          # material ID tag – lightweight concrete layer
set IDconcU2 2;          # material ID tag – normal-weight concrete layer
set IDreinf 4;           # material ID tag – reinforcement

# -----
# lightweight concrete layer properties

set fc1 -70;             # lightweight concrete layer compressive Strength
set Ec1 48498;           # lightweight concrete layer Elastic Modulus
set eps1U1 -0.002;      # strain at maximum strength of lightweight concrete layer
set eps2U1 -0.004;     # strain at ultimate stress of lightweight concrete layer

# -----
# Normal-weight concrete layer
set fc2 -398;            # Normal-weight concrete layer compressive Strength
set Ec2 247095;         # Normal-weight concrete layer Elastic
Modulus
set eps1U2 -0.002;     # strain at maximum strength of normal-weight concrete layer
set eps2U2 -0.004;     # strain at ultimate stress of normal-weight concrete layer

# -----
# Steel properties

set Fy 3700;            # Steel yield stress
set Es 2100000;         # modulus of steel
set Bs 0.027;           # strain-hardening ratio
set R0 10;              # control the transition from elastic to plastic branches
set cR1 0.925;          # control the transition from elastic to plastic branches
set cR2 0.15;          # control the transition from elastic to plastic branches

#-----

uniaxialMaterial Concrete04 $IDconcU1 $fc1U1 $eps1U1 $eps2U1 $Ec1;
# build lightweight concrete layer material
uniaxialMaterial Concrete04 $IDconcU2 $fc1U2 $eps1U2 $eps2U2 $Ec2;
# build normal-weight concrete layer material
uniaxialMaterial Steel02 $IDreinf $Fy $Es $Bs $R0 $cR1 $cR2;
# build reinforcement material

```

```

# FIBER SECTION properties -----
section Fiber 1 {

    fiber -9.975 0.0    1.5          $IDconcU1
    fiber -9.925 0.0    1.5          $IDconcU1
    fiber -9.875 0.0    1.5          $IDconcU1
    fiber -9.825 0.0    1.5          $IDconcU1
    fiber -9.775 0.0    1.5          $IDconcU1
    ...
    fiber -0.175 0.0    1.5          $IDconcU1
    fiber -0.125 0.0    1.5          $IDconcU1
    fiber -0.075 0.0    1.5          $IDconcU1
    fiber -0.025 0.0    1.5          $IDconcU1

    fiber 9.975 0.0    1.5          $IDconcU2
    fiber 9.925 0.0    1.5          $IDconcU2
    fiber 9.875 0.0    1.5          $IDconcU2
    ...
    fiber 0.175 0.0    1.5          $IDconcU2
    fiber 0.125 0.0    1.5          $IDconcU2
    fiber 0.075 0.0    1.5          $IDconcU2
    fiber 0.025 0.0    1.5          $IDconcU2

    # tensile steel reinforcement
    fiber 7.600 0.0    $barAreaCol    $IDreinf
}

# define geometric transformation: performs a linear geometric transformation of
# beam
# stiffness and resisting force from the basic system to the global-coordinate
# system
set ColTransfTag1 1;          # associate a tag to column transformation
geomTransf Linear $ColTransfTag1;

# element connectivity:
set numIntgrPts 6;          # number of integration points for force-based
# element
set integration1 "Legendre $ColSecTag1 $numIntgrPts";
element forceBeamColumn 1 1 2 $ColTransfTag1 $integration1;
element forceBeamColumn 2 2 3 $ColTransfTag1 $integration1;
element forceBeamColumn 3 3 4 $ColTransfTag1 $integration1;
element forceBeamColumn 4 4 5 $ColTransfTag1 $integration1;

```

```

element forceBeamColumn 5 5 6 $ColTransfTag1 $integration1;
element forceBeamColumn 6 6 7 $ColTransfTag1 $integration1;

```

```
puts "Model Built"
```

```

# STATIC ANALYSIS -----
#
# we need to set up parameters that are particular to the model
set IDctrlNode 3;          # node where displacement is read for displacement
control
set IDctrlDOF 1; # degree of freedom of displacement read for displacement
control

# create load pattern for lateral pushover load
set Hload 1;
pattern Plain 2 Linear {          # define load pattern -- generalized
    load 3 $Hload 0.0 0.0;
    load 5 $Hload 0.0 0.0;
}

# Set up analysis parameters -----

# CONSTRAINTS handler -- Determines how the constraint equations are enforced
in the analysis
# Plain Constraints -- Removes constrained degrees of freedom from the system of
equations (only for homogeneous equations)
constraints Plain

# DOF NUMBERER (number the degrees of freedom in the domain):
# determines the mapping between equation numbers and degrees-of-freedom
# Plain -- Uses the numbering provided by the user
numberer Plain

# SYSTEM -----

# Linear Equation Solvers (how to store and solve the system of equations in the
analysis)
# -- provide the solution of the linear system of equations  $Ku = P$ . Each solver is
tailored to a specific matrix topology.
# BandGeneral -- Direct solver for banded unsymmetric matrices

system BandGeneral

```

```

# TEST: # convergence test to -----
#                               Convergence                               TEST
(http://opensees.berkeley.edu/OpenSees/manuals/usermanual/360.htm)
# -- Accept the current state of the domain as being on the converged solution path
# -- determine if convergence has been achieved at the end of an iteration step
#   EnergyIncr-- Specifies a tolerance on the inner product of the unbalanced load
and displacement increments at the current iteration
set Tol 1.e-4;           # Convergence Test: tolerance
set maxNumIter 3000;    # Convergence Test: maximum number of iterations that
will be performed before "failure to converge" is returned
set printFlag 0;       # Convergence Test: flag used to print information on
convergence (optional) # 1: print information on each step;
set TestType EnergyIncr; # Convergence-test type
test $TestType $Tol $maxNumIter $printFlag;

# Solution ALGORITHM: -- Iterate from the last time step to the current
#   Newton -- Uses the tangent at the current iteration to iterate to convergence
algorithm Newton;

# ANALYSIS -- defines what type of analysis is to be performed
#   Static Analysis -- solves the KU=R problem, without the mass or damping
matrices.
analysis Static

# Define RECORDERS -----

recorder Node -file DFree3.out -time -node $IDctrlNode -dof 1 2 3 disp;
# displacements of free nodes

recorder Node -file DFree4.out -time -node 4 -dof 1 2 3 disp;
# displacements of free nodes

recorder Element -file FCo1.out -time -ele 1 globalForce;

recorder Element -file concrete_edgeSup.out -ele 3 section 1 fiber -9.975 0.0 1
stressStrain

recorder Element -file concrete_edgeInf.out -ele 3 section 1 fiber 9.975 0.0 2
stressStrain

recorder Element -file steel_layer.out -ele 3 section 1 fiber 7.600 0.0 4
stressStrain

```

```
# Perform Static Pushover Analysis
set Incr 1000

# Static INTEGRATOR: -- determine the next time step for an analysis

# DisplacementControl -- Specifies the incremental displacement at a specified
DOF in the domain

    integrator DisplacementControl $IDctrlNode $IDctrlDOF -0.01

    analyze $Incr
    print node $IDctrlNode

puts "Done!\a"
```

#### 8.4. Monotonic load test in RSC specimens

This section shows the results and failure modes of the monotonic load test developed on reinforced stratified concrete specimens. Two beams of two different mixtures (SCG and SCS) were tested.



Figure 8-5: Monotonic load test set up



Figure 8-6: Failure mode SCG-1 specimen

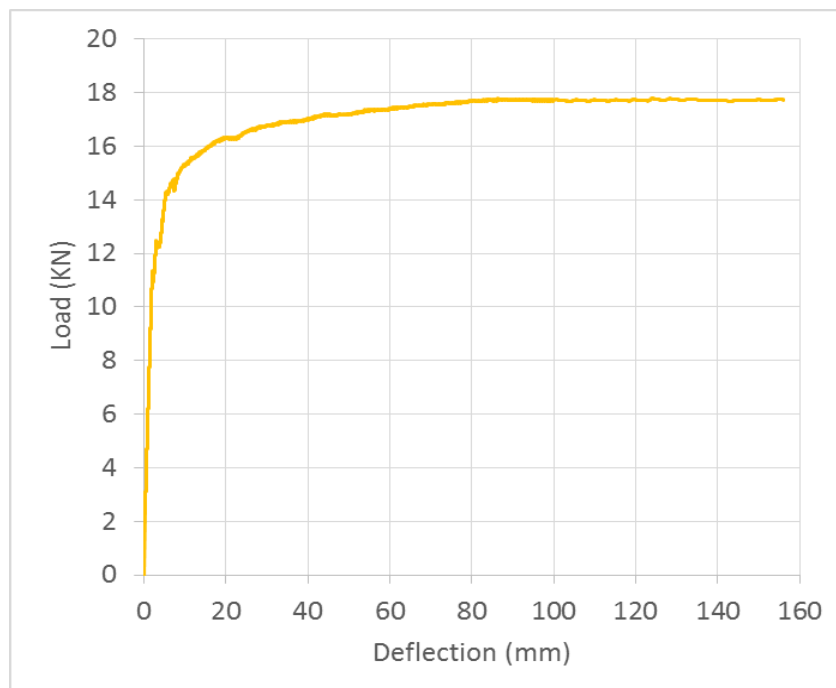


Figure 8-7: Load-deflection curve SCG-1 specimen



Figure 8-8: Failure mode SCG-2 specimen

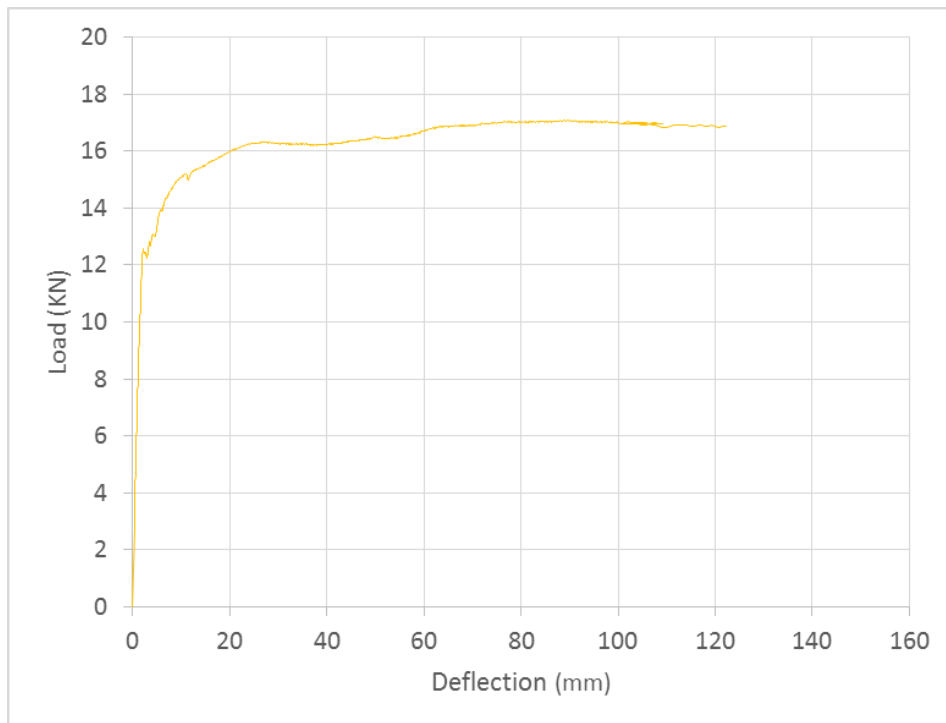


Figure 8-9: Load-deflection curve SCG-2 specimen



Figure 8-10: Failure mode SCS-1 specimen

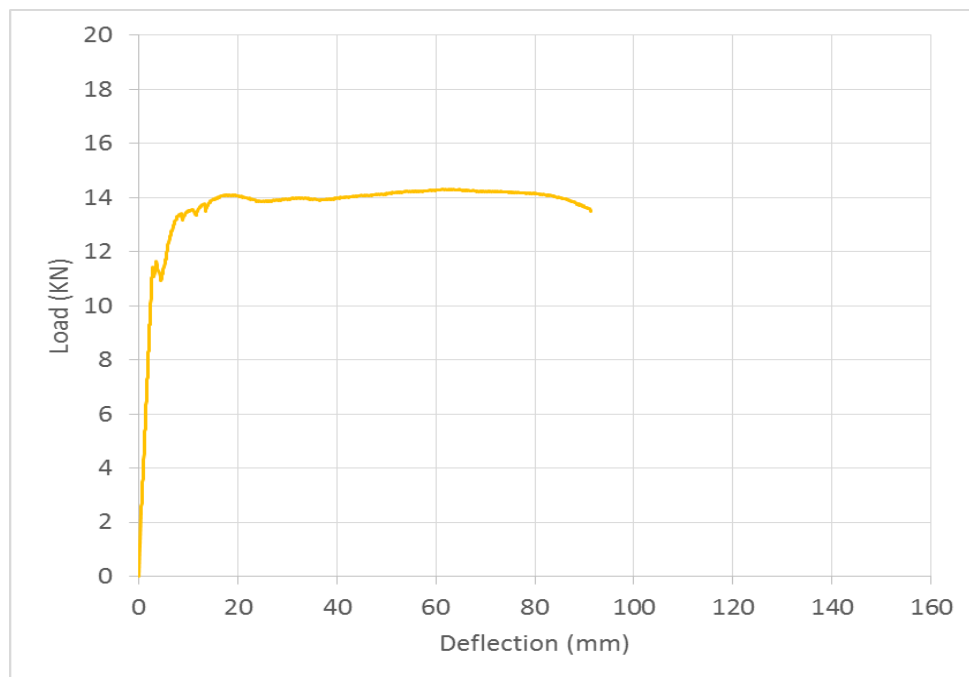


Figure 8-11: Load-deflection curve SCS-1 specimen



Figure 8-12: Failure mode SCS-1 specimen

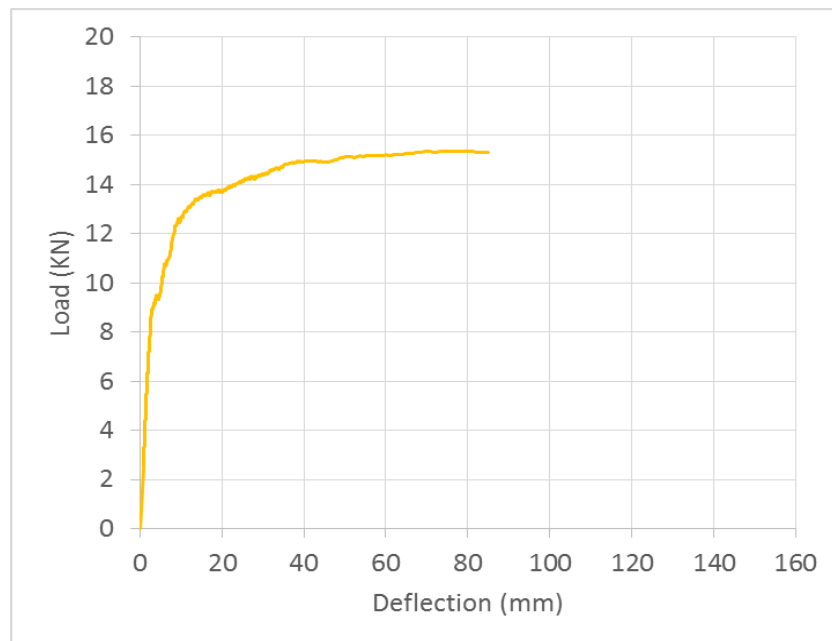


Figure 8-13: Load-deflection curve SCS-1 specimen